

## CHAPTER 4

### RESULTS AND DISCUSSION

#### 4.1 Morphology of the toner and the carrier particles

The scanning electron micrographs of the different shapes of toners, irregular shape (KT-16a) and spherical shape (N-09S), are shown in Figure 4-1. The surface of the spherical-shaped toner is smoother than the surface of irregular-shaped toner.

The scanning electron micrographs in Figure 4-2 shows the different carrier particles of the ferrite carrier (F-200) and the steel carrier (TSV-200). The shape of F-200 carrier is more spherical than the other.

#### 4.2 Toner charge dependence on the mixing force

The KT-16a toner charge to mass ratio ( $q/m$ ) was dependent on the mixing force (rotation speed) of different carriers, F-200 carrier and TSV-200 carrier. As a result, the developers were mixed together for 3 wt% (concentration) at rotating speeds 400, 600, 800, 1000, 1200, and 1400 rpm as shown in Figures 4-4 to 4-7.

Figures 4-4 and 4-6 show the relationship between the  $q/m$  values and the rotating time. The KT-16a toner  $q/m$  at rotating speeds of 400, 600, 800, and 1000 rpm were not stable during 30 to 120 seconds. The  $q/m$  values of KT-16a toner increased with an increase in the rotating time and reached a saturation value at 240 seconds. The  $q/m$  values of KT-16a toner and TSV-200 carrier were higher than those of KT-16a toner and F-200 carrier at several speeds. But, the developer with F-200 carrier had a wide range of the  $q/m$  values more than the other. During other rotating speeds, 1200 and 1400 rpm, the  $q/m$  values increased to a maximum value at 60 seconds and then immediately decreased. The  $q/m$  values of KT-16a toner and TSV-200 carrier were decreased rapidly than the other. The deformation of the toner with steel carrier was severe than the toner with ferrite carrier. This is shown in the Figure 4-12.

Figures 4-5 and 4-7 show the curves of the maximum toner charge  $(q/m)_{\max}$  in relation to the rotating speed (rpm), the acceleration ( $m/s^2$ ), and the mixing force (N). The acceleration was calculated from the rpm, and the calculation of the mixing force could be multiplied by the weight of toner and the acceleration. The lines of these relations showed a similar tendency, especially, the acceleration line and the mixing force line were almost the same line. Therefore, the  $q/m(\max)$  values increased with an increasing rotating speed (rpm).

The N-O9S toner was mixed with each type of ferrite carrier, F-200, including steel carrier, TSV-200. The toner-to-carrier wt% ratio was five. After the uncharged toner and carrier were combined in a glass cell (24 mm in diameter), the rotating speeds were adjusted to 400, 600, 800, 1000, 1200, and 1400 rpm. The toner charge-to-mass ratio was plotted as a function of time for several rotating speeds in Figures 4-8 and 4-10. The curves of the two developers, for the KT-16a toner with the F-200 carrier and the TSV-200 carrier, showed the same tendency to increase to a constant value.

Figures 4-9 and 4-11 show the relation between N-O9S toner  $q/m(\max)$  values in relation to the rotating speed (rpm), the acceleration ( $m/s^2$ ), and the mixing force (N), respectively. The trend of the lines is similar to those of Figures 4-5 and 4-7.

In conclusion, the tribocharging ( $q/m$ ) of the developers begins with a rapid increase and then reaches a saturation value at 240 seconds with rotating speeds of 400 to 1000 rpm. For these speeds, the  $q/m$  values and saturation values increased with increasing rotating speeds.<sup>6</sup> The increase in  $q/m$  values and saturation values were due to an increase in the mixing force, an increase in the contact area and an increase in the friction between the toners and carriers. As a result, the toner charge-to-mass ratio ( $q/m$ ) also increased.

During high speeds of 1200 and 1400 rpm, the curves showed the maximum  $q/m$  values. After several minutes, the  $q/m$  values then decreased. This decrease was caused by the charge control agent (CCA), which may have fallen out of the toner component and was removed to the carrier surface during contact. This is so called "Carrier contamination with CCA", when the CCA surfaces were in contact, the charges could not be exchanged. When toners without CCA were used, no charge occurred; therefore, the  $q/m$  values were low.<sup>17</sup> Another reason was in accordance

with the literature of the toner impaction, which meant the permanency of toner particles to the carrier surface. This affect is caused by reducing the  $q/m$  value. Since the contaminated area of the carrier beads could not provide charging sites for free toner particles.<sup>7</sup> From the SEM photographs (Figure 4-12) show the deformation of toners with the carriers. This deformation led to lowering the effective charging of toners.

The calculation of the force from the rotating speed (rpm) in the mixing roller as follows:

$$F = ma \quad (4-1)$$

where  $F$  = the force of rotating speed,  $m$  = weight of the toner, and  $a$  = the acceleration of gravity rotation.

Let assume that the toner particles are spherical, in which the  $m$  value can be calculated as:

$$m = \left( \frac{4}{3} \pi r_t^3 \rho_t \right) M_t \quad (4-2)$$

where  $m$  = weight of the toner,  $r_t$  = radius of the toner,  $\rho_t$  = density of the toner, and  $M_t$  = number of the toners.

The acceleration ( $m/s^2$ ) can be calculated from the rotating speed (rpm) of an MS1 Minishaker (shown in Figure 4-3), as follows:

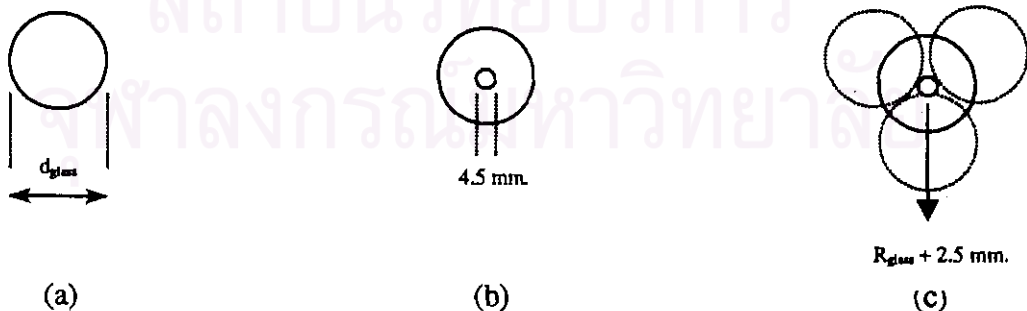


Figure 4-3 A model of rotating by the MS1 Minishaker : (a) glass cell (diameter of the glass cell, 24 mm), (b) before rotating, and (c) while rotating of the glass cell

The centrifugal force can be computed from the following equation.

$$\text{Centrifugal force by rotating} = (r + 2.5) \omega^2 \text{ m/s}^2 \quad (4-3)$$

where  $r$  = radius of glass cell and  $\omega$  = angular velocity

The force of rotating speed is calculated from one molecule of the toner. Example of the calculation is shown below:

The force of rotating speed at 400 rpm.

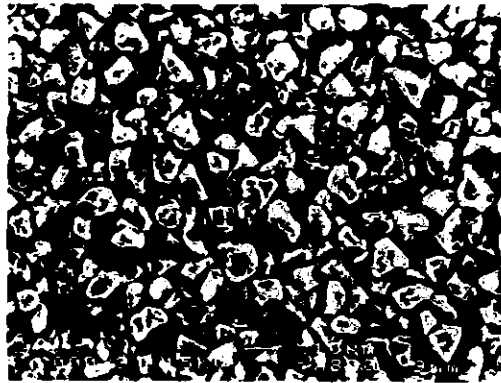
$$F_{400 \text{ rpm}} = \left[ \frac{4}{3} \pi (4 \times 10^{-6})^3 (1.2 \times 10^{-3}) \right] \left[ \left( \frac{12 + 2.5}{1000} \right) \left( \frac{400}{60} \times 2\pi \right)^2 \right]$$

$$= 1.72 \times 10^{-16} \text{ N}$$

Table 4-1 : The relationship of the rotating speed (rpm), the acceleration ( $\text{m/s}^2$ ), and the mixing force (N)

Rotating speed (rpm)	Acceleration ( $\text{m/s}^2$ )	Mixing force ( $\times 10^{-16}$ N)
400	25.44	1.72
600	57.24	3.87
800	101.77	6.88
1000	159.01	10.75
1200	228.97	15.47
1400	311.66	21.06

Table 4-1 shows the relationship of the rotating speed (rpm), the acceleration ( $\text{m/s}^2$ ), and the mixing force (N). The mixing force increases with increasing the rotating speed.



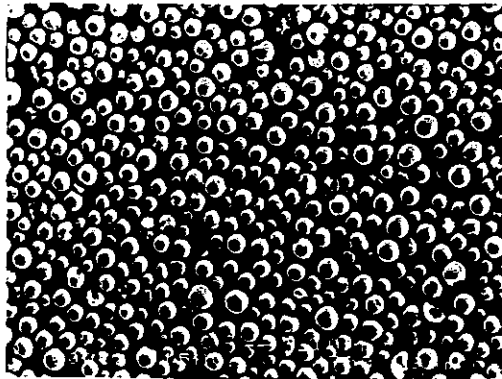
(a)



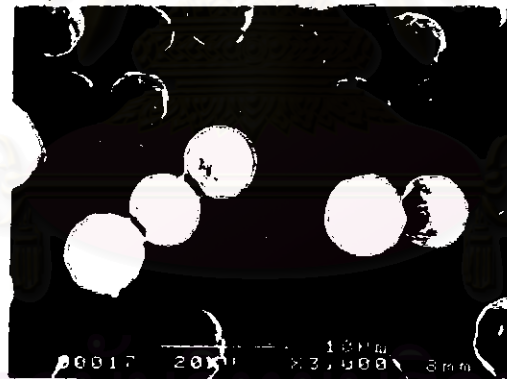
(b)



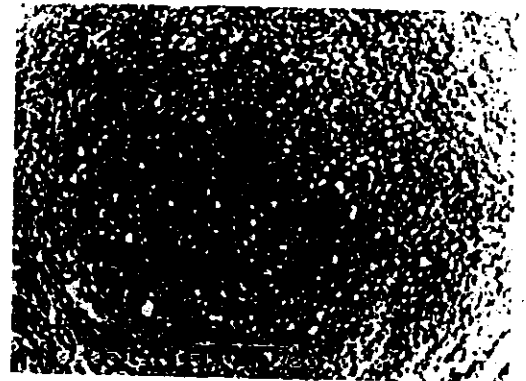
(c)



(d)

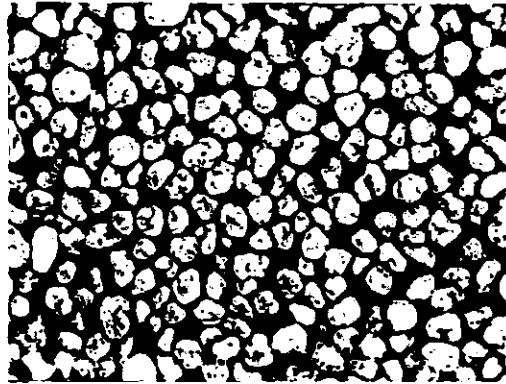


(e)



(f)

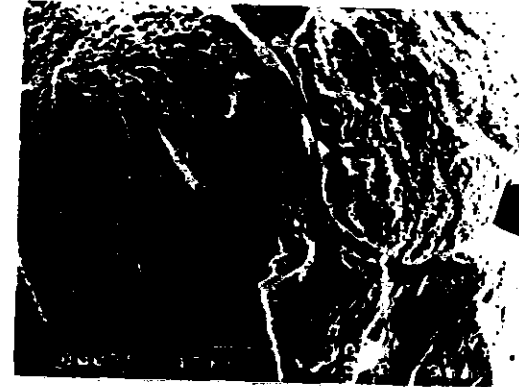
Figure 4-1 Scanning electron micrographs of the toners : (a) KT-16a (x800), (b) KT-16a (x3000), (c) KT-16a (x13000), (d) N-O9S (x700), (e) N-O9S (x3000), and (f) N-O9S (x20000)



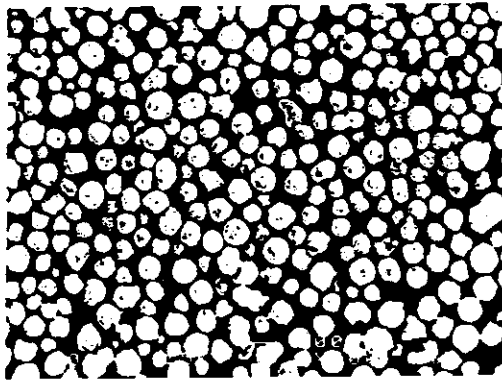
(a)



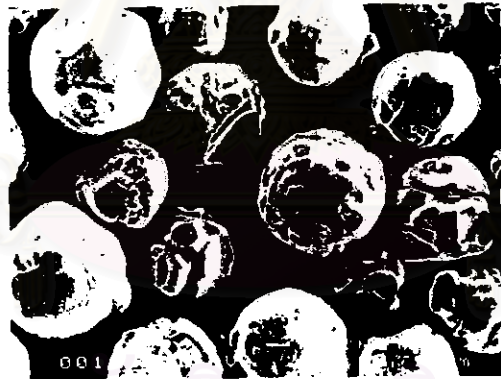
(b)



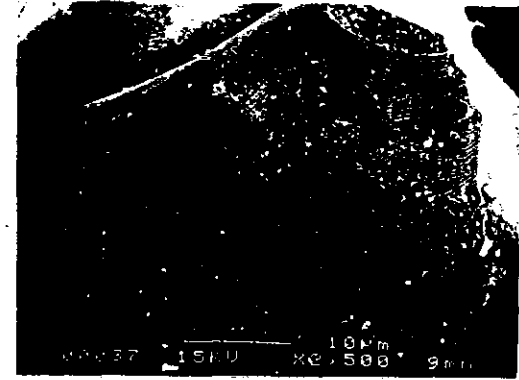
(c)



(d)



(e)



(f)

Figure 4-2 Scanning electron micrographs of the carriers : (a) TSV-200 (x95), (b) TSV-200 (x350), (c) TSV-200 (x2500), (d) F-200 (x100), (e) F-200 (x500), and (f) F-200 (x2500)

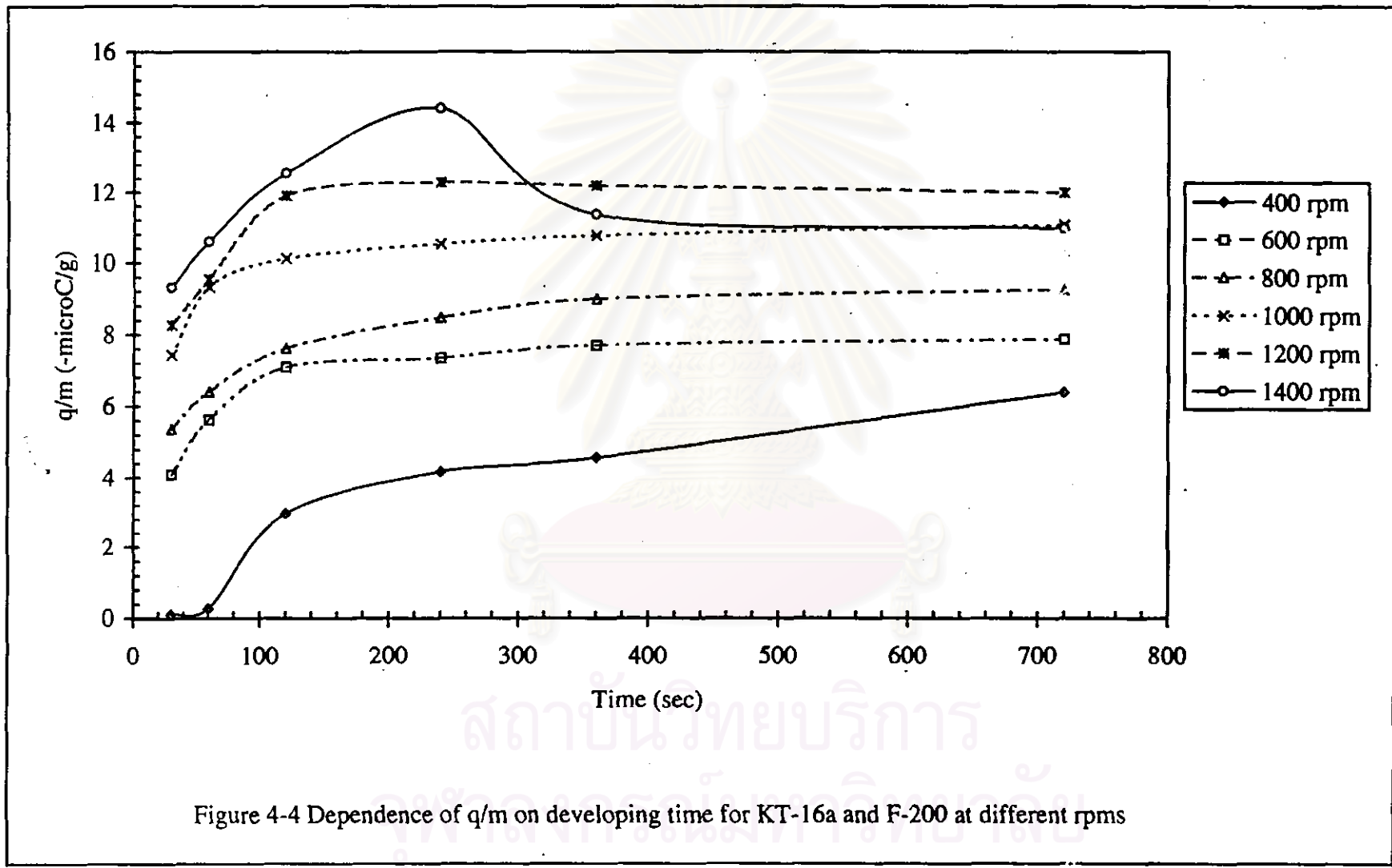


Figure 4-4 Dependence of  $q/m$  on developing time for KT-16a and F-200 at different rpm

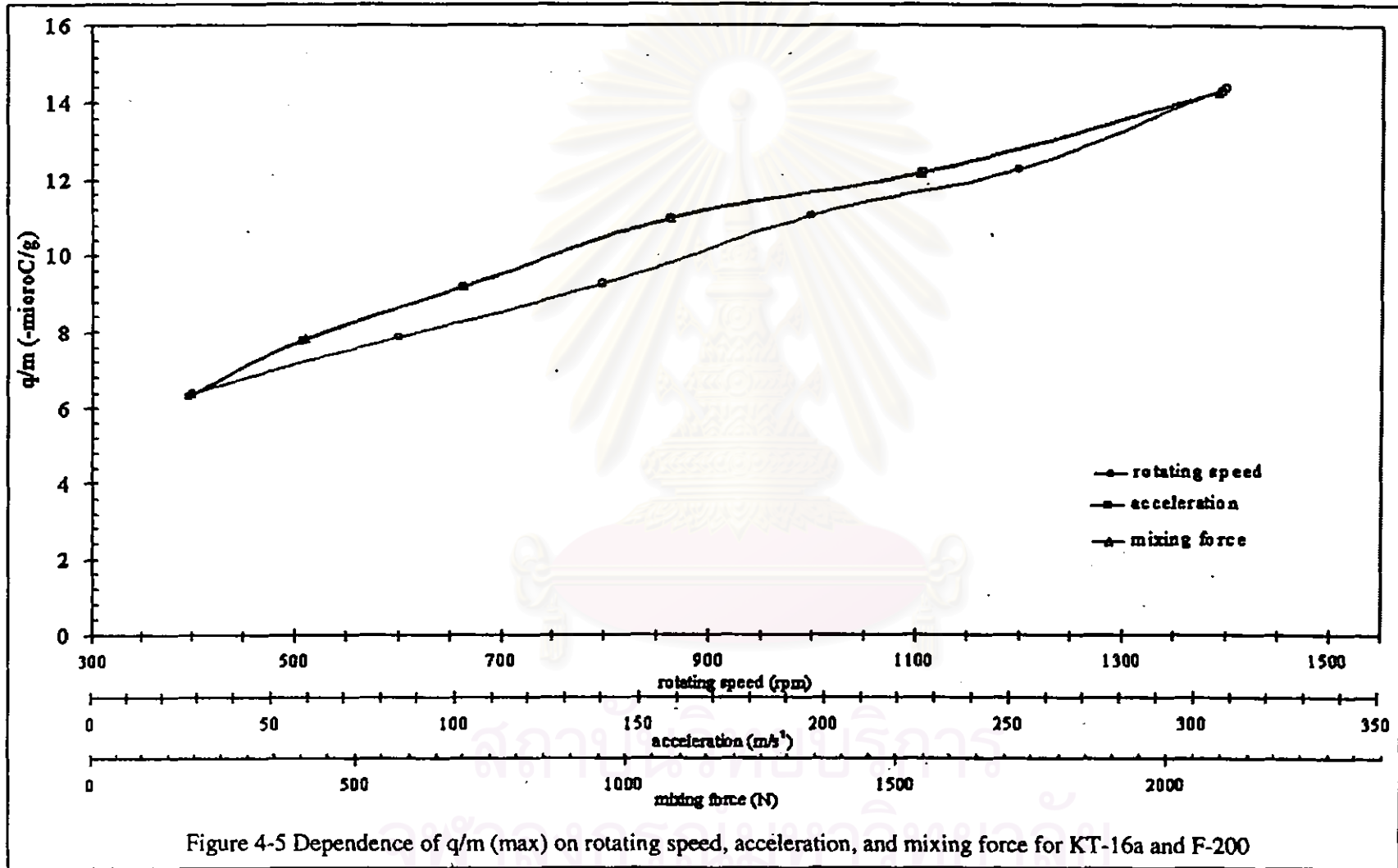


Figure 4-5 Dependence of  $q/m$  (max) on rotating speed, acceleration, and mixing force for KT-16a and F-200



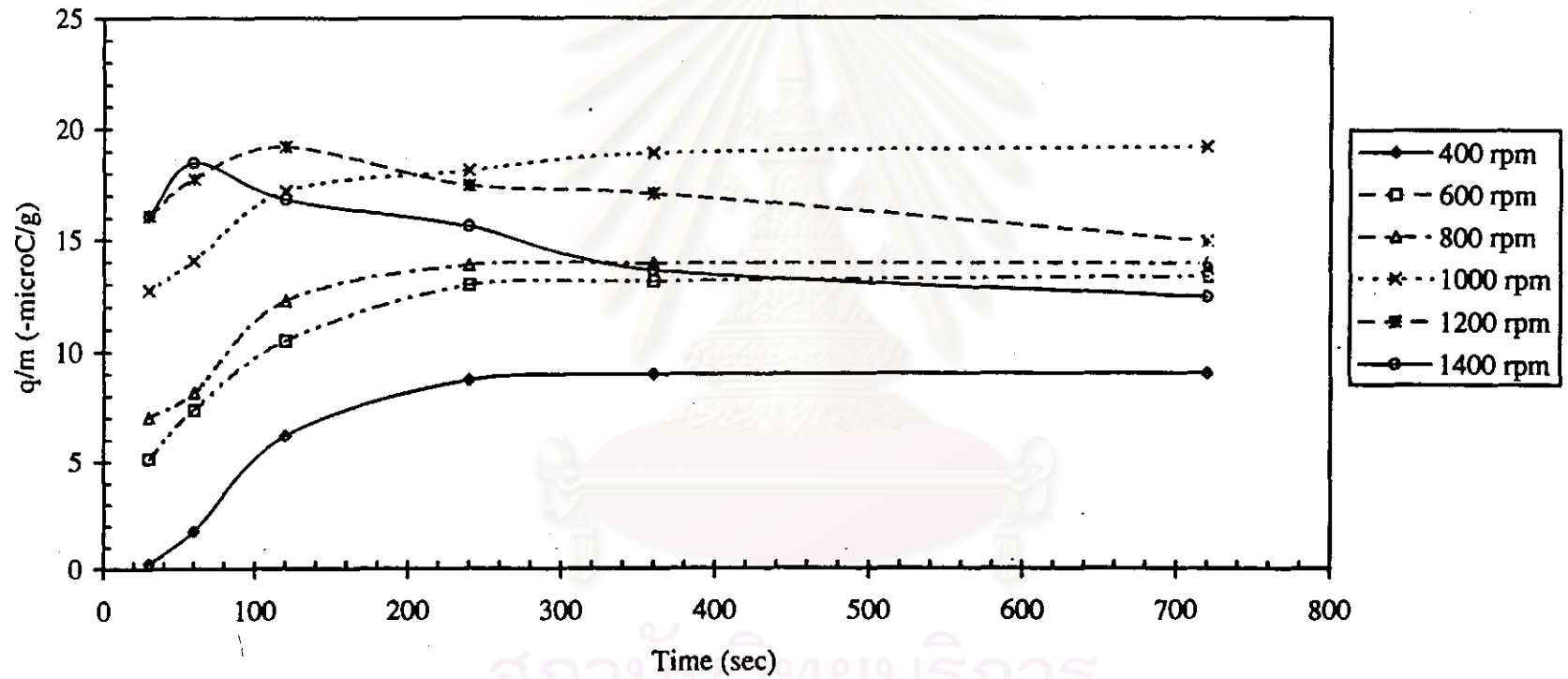


Figure 4-6 Dependence of  $q/m$  on developing time for KT-16a and TSV-200 at different rpms

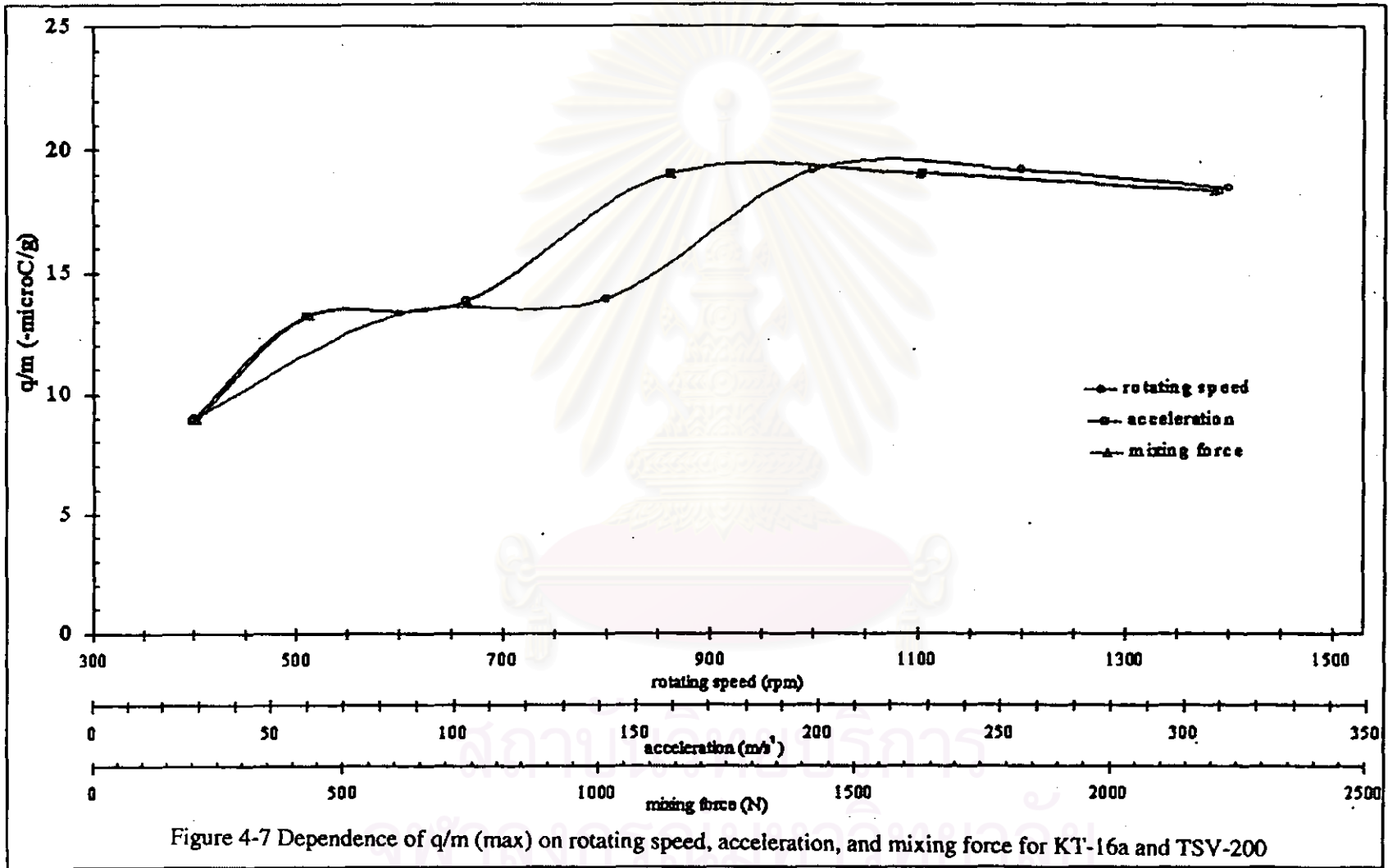


Figure 4-7 Dependence of  $q/m$  (max) on rotating speed, acceleration, and mixing force for KT-16a and TSV-200

I 11946999

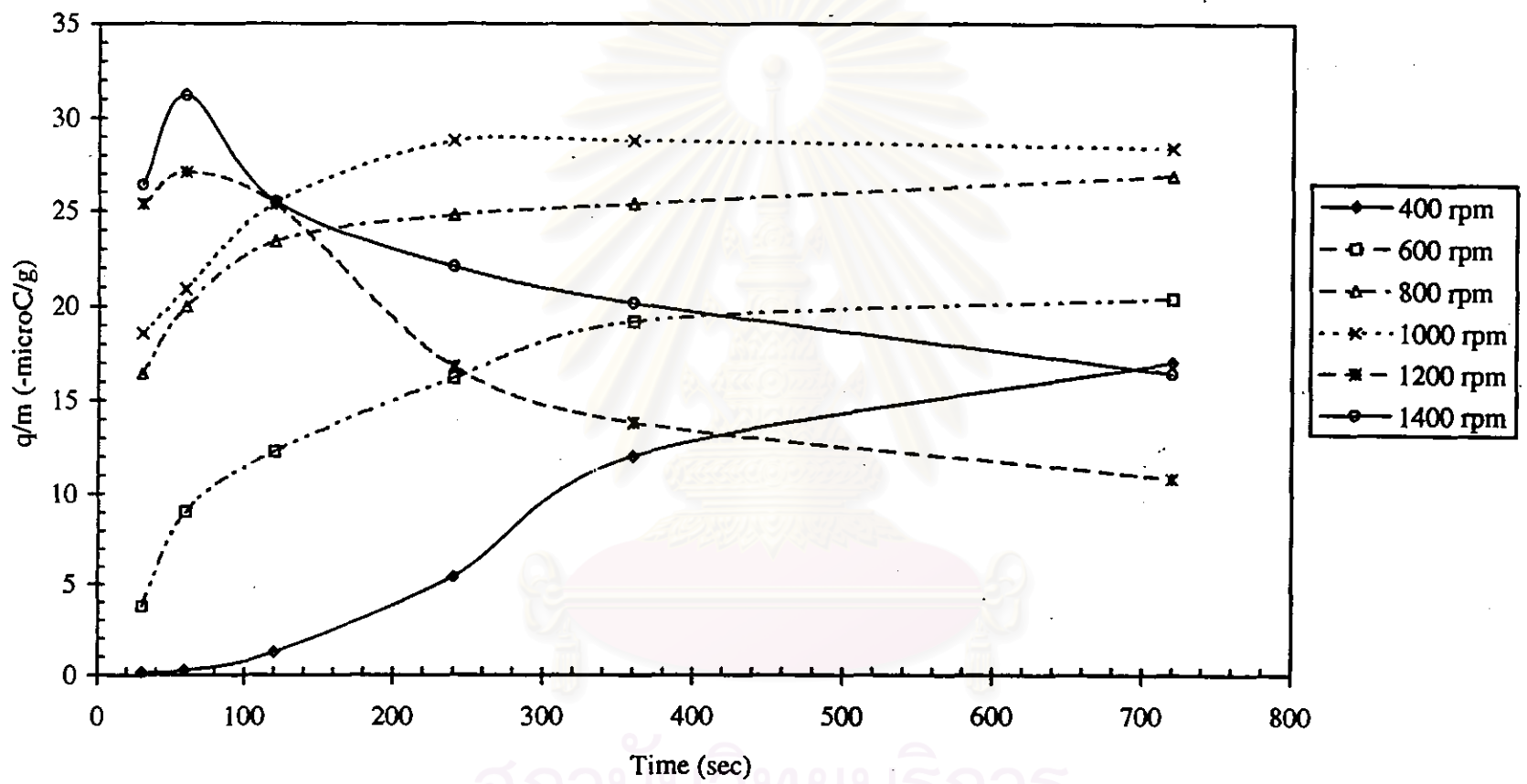
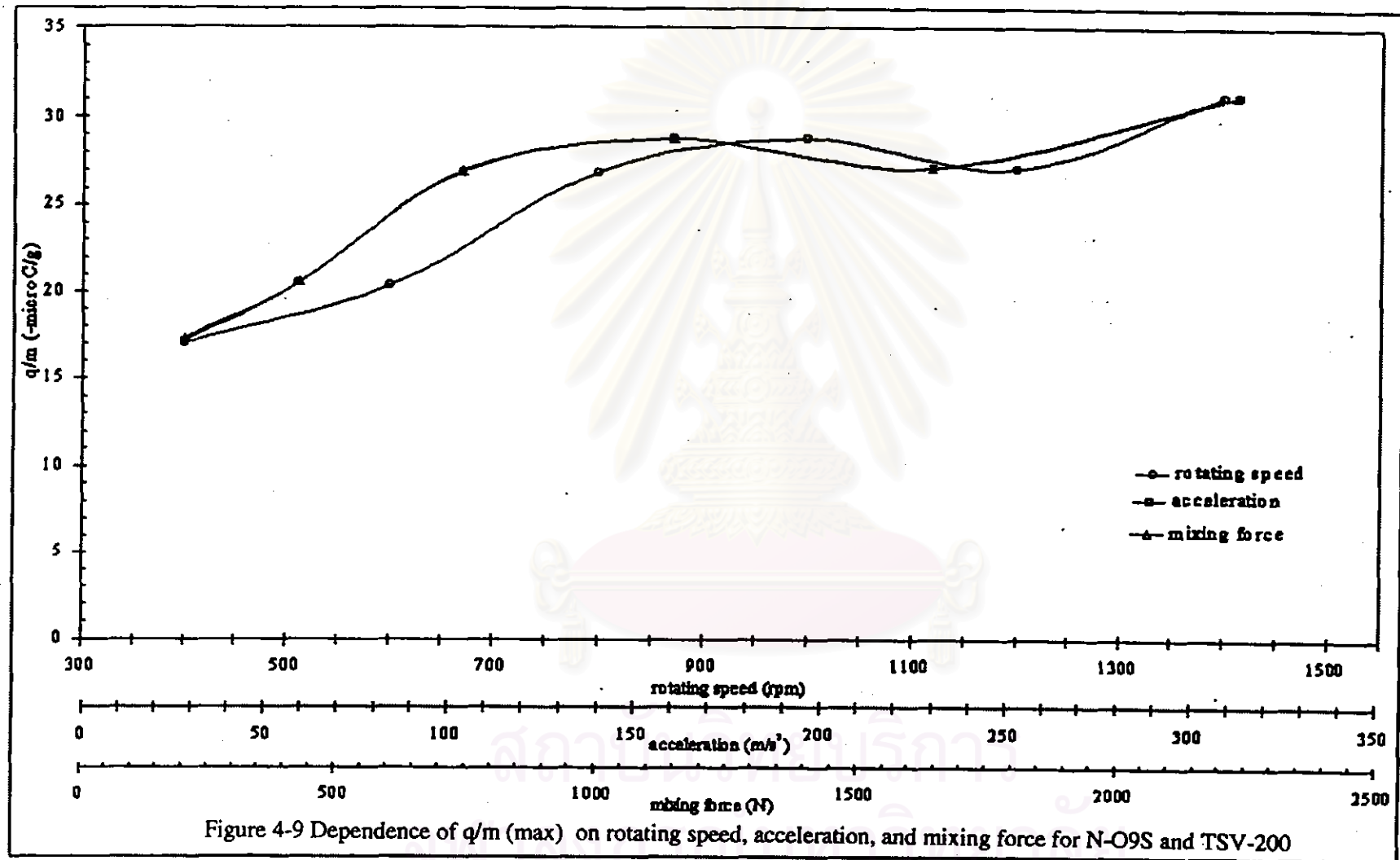


Figure 4-8 Dependence of  $q/m$  on developing time for N-O9S and TSV-200 at different rpms

สถาบันวิทยบริการ  
คลังสารนิพนธ์



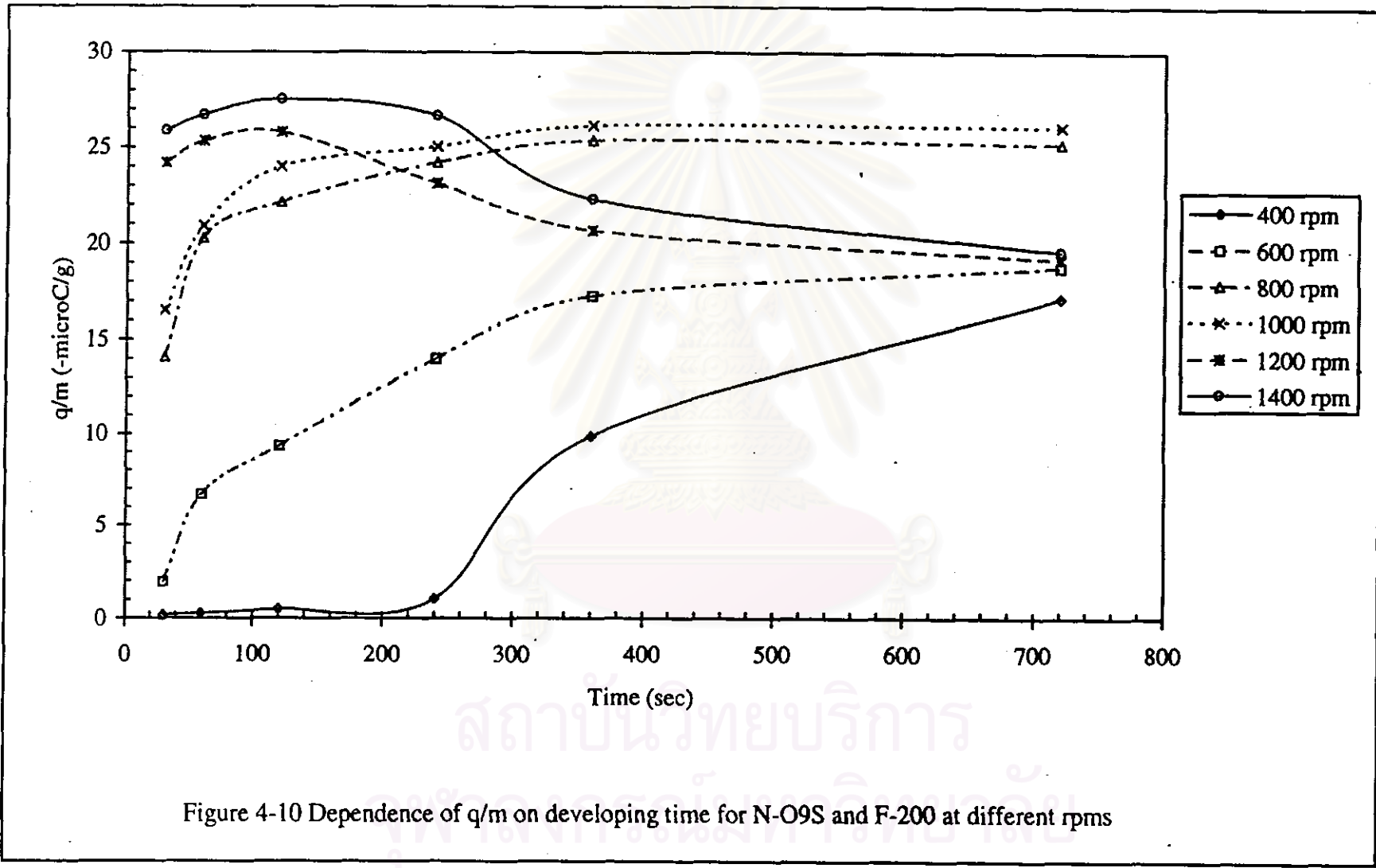


Figure 4-10 Dependence of  $q/m$  on developing time for N-O9S and F-200 at different rpms

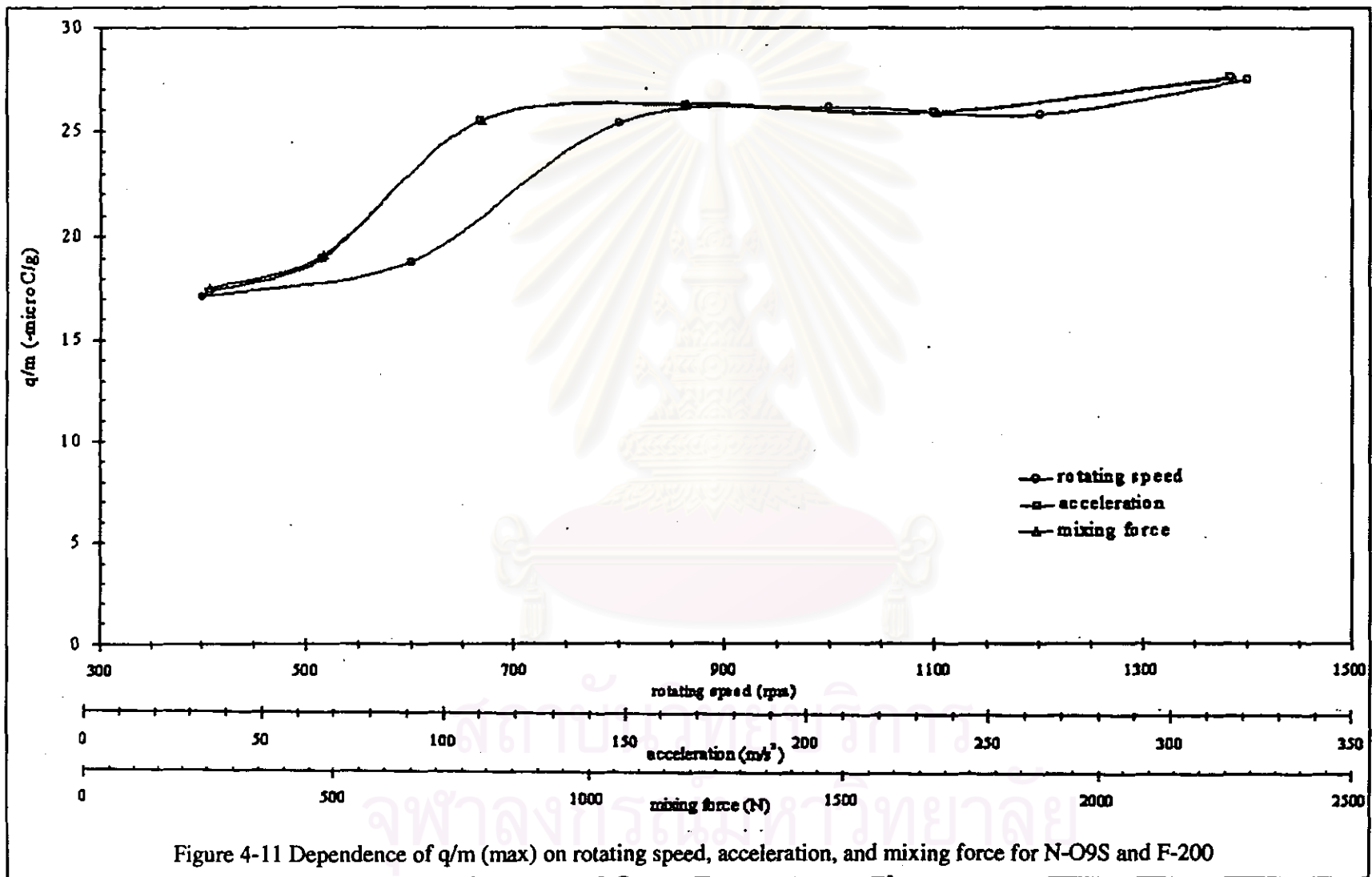


Figure 4-11 Dependence of  $q/m$  (max) on rotating speed, acceleration, and mixing force for N-O9S and F-200

### 4.3 Morphology of the deformation of KT-16a toner

The SEM photographs (Figure 4-12) show the deformation of KT-16a toner at high rotating speed with different carriers, F-200 carrier and TSV-200 carrier. The toners are crushed with the carriers and then adhered on the carrier surface.

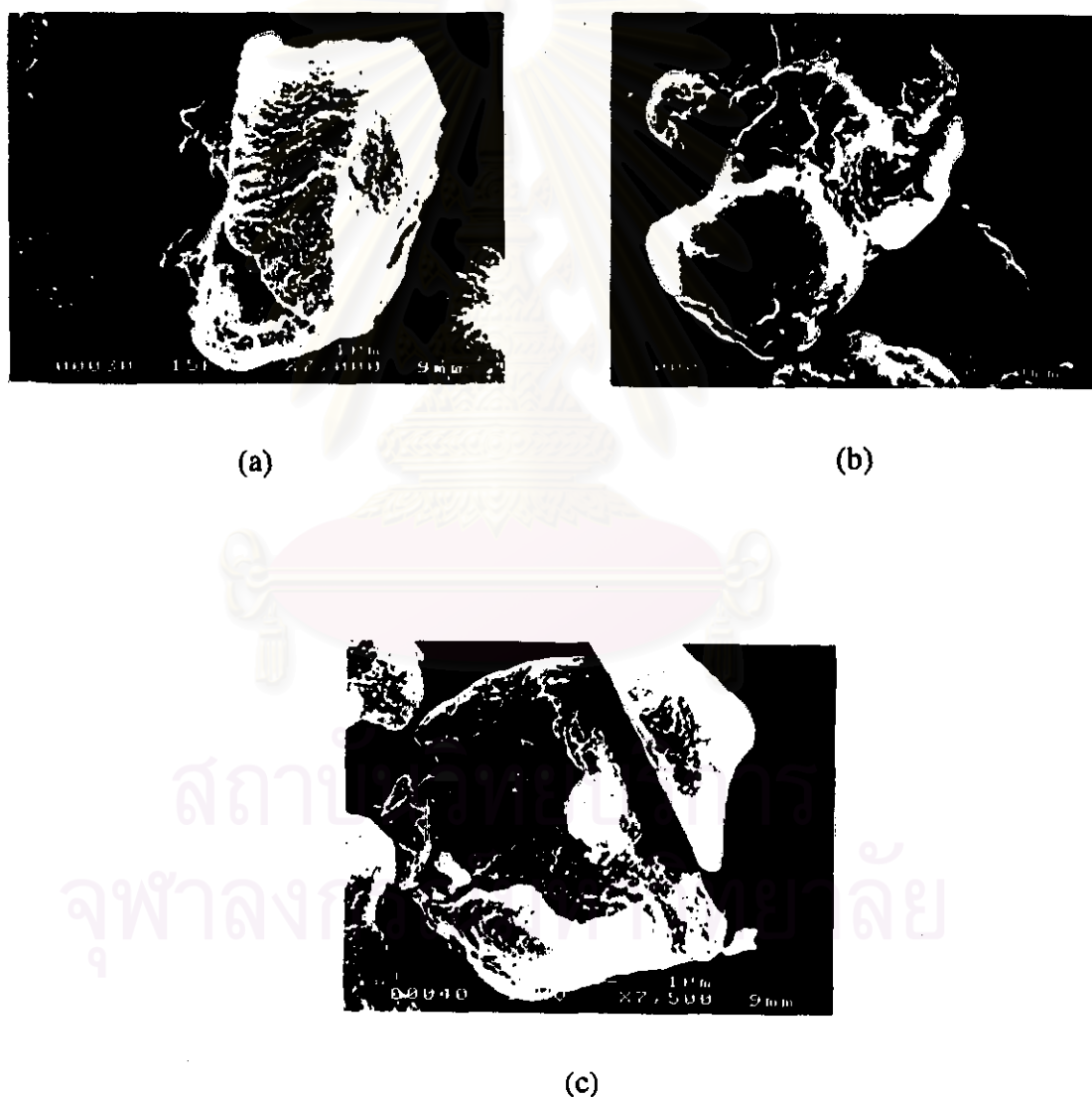


Figure 4-12 Scanning electron micrographs of KT-16a toner : (a) before rotation, (b) rotation speed at 1200 rpm with TSV-200 carrier, and (c) rotation speed at 1400 rpm with F-200 carrier

#### 4.4 Toner charge dependence on the toner concentration (wt%)

The toner, KT-16a, was mixed with two types of carriers, F-200 and TSV-200. These carriers were prepared by various concentrations comprising 1, 2, 3, 5, 7, and 10 wt%, at rotating speeds of the glass cell (24 mm in diameter) of 600, 800, and 1000 rpm. The  $q/m$  curves for the KT-16a toner mixed with the F-200 carrier were plotted in relation to the rotating times and various rotating speeds in Figures 4-14 to 4-16, respectively. The curves of these rotation speeds showed a similar tendency. For toner concentrations of 2, 3, 5, 7, and 10 wt%, the amount of the toner charge changed rapidly when the rotation of the developer was continued for longer than 120 seconds. The values of the toner charge then approached a quasistatic value that changes very slowly and was defined as the maximum charge.<sup>6</sup> For the curves of these toner concentrations, an equilibrium charge values at lower speed had a wide range more than the higher speed. But for 1 wt%, the  $q/m$  values increased to the maximum  $q/m$  value and then decreased after a few minutes. The toners were attached on the glass wall, when the movement of the glass cell was continued. Especially, the toners were strongly attached at the high speed. Then, most of the toners were lost and were not measured by blow-off method. So, the  $q/m$  values were rapidly decreased.

Figures 4-17 to 4-19 show the relationship between the  $q/m$  values of the developer, KT-16a toner and TSV-200 carrier, and the rotating time for varied rotating speeds of 600, 800, and 1000 rpm, respectively. The toner charge-to-mass ratio of 1 wt% at 800 and 1000 rpm had very low values, which were affected by the same phenomenon occurred to the KT-16a toner and F-200 carrier at 1 wt%. The characteristics of the coverage for the KT-16a toner on the TSV-200 carrier surface at the same wt% were resemble those of the KT-16a toner and F-200 carrier. Consequently, the toners had the same effective charging mechanism.

Figures 4-20 and 4-22 show the curves of  $q/m(\max)$  in relation to the toner concentration (wt%) of KT-16a toner mixed with each of the carriers, F-200 carrier and TSV-200 carrier. The  $q/m(\max)$  values decreased with an increase in the toner concentration from 1 wt% to 10 wt%. The coverage of toners on a carrier surface is higher and more than one layer, when the toner concentration is higher. So, the toner charge decreases with increasing toner concentration, and there are free toners if the



coverage is more than one layer.<sup>18</sup> These results showed the similar tendency as the relation curves between the  $q/m$  values and the rotating time.

Figures 4-21 and 4-23 display two measurements of the sample. One measurement is for the KT-16a toner and F-200 carrier and the other is for KT-16a toner and TSV-200 carrier. The figures were plotted between the inverse  $q/m$  (max) values and the toner concentration (wt%). At each intermediate toner concentration, sufficient charging is made to ensure that the developer reaches a quasistatic charge state for that particular toner concentration. These curves show that the maximum toner mass-to-charge ratio  $(m/q)_{\text{max}}$  increases with an increasing wt% of toner. This increase occurs with all of the rotating speeds in this experiment.

For all of the developers, the time constant increased and the toner charge decreased with an increase in the toner concentration of the developer. During the rotating speeds for the toner concentration of 1 wt%, the  $q/m$  values increased to the highest value and then decreased. This occurrence is a result of the toner particles being attached on the glass wall, which were not removed during sampling and measuring for the blow off method. At high toner concentration, which was under the condition of  $N_t > N_c$ ,<sup>18</sup> the toner coverage on a carrier surface is higher and occupies more than one layer. The outer layer has some free toner particles that cannot be charged by rubbing with the carrier particles. So the  $q/m$  values were decreased with an increase in toner concentration (wt%), which was in agreement with those reported by Gutman and Hartmann,<sup>6</sup> and Schein.<sup>23</sup>

The calculation of the relationship between the toner concentration (wt%) and the coverage (%) is shown below.

Let's assume that toner particles and carrier particles are in a spherical shape, and the toner concentration (wt%) is  $x\%$ .

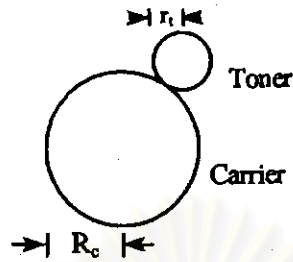


Figure 4-13 A model of the coverage of toner on carrier surface

$$\text{Weight of carrier} : \frac{4}{3} \pi R_c^3 \rho_c$$

$$\text{Weight of toner} : \frac{4}{3} \pi r_t^3 \rho_t$$

$$\frac{x}{100} = \frac{\left( \frac{4}{3} \pi r_t^3 \rho_t \right) M_t}{\left( \frac{4}{3} \pi R_c^3 \rho_c \right) M_c + \left( \frac{4}{3} \pi r_t^3 \rho_t \right) M_t} \quad (4-4)$$

where  $R_c$  = radius of the carrier,  $r_t$  = radius of the toner,  $\rho_c$  = density of the carrier,  $\rho_t$  = density of the toner,  $M_c$  = number of the carriers, and  $M_t$  = number of the toners

$$\frac{x}{100} = \frac{r_t^3 \rho_t}{R_c^3 \rho_c \frac{M_c}{M_t} + r_t^3 \rho_t} \quad (4-5)$$

$$\frac{M_c}{M_t} = \frac{\frac{100}{x} r_t^3 \rho_t - r_t^3 \rho_t}{R_c^3 \rho_c} \quad (4-6)$$

$$\text{Coverage} = \frac{(\pi r_t^2) M_t}{(4\pi R_c^2) M_c} \quad (4-7)$$

$$= \left( \frac{r_t^2}{4R_c^2} \right) \left( \frac{M_t}{M_c} \right) \quad (4-8)$$

Substitute ( $M_t/M_c$ ) from equation (4-6)

$$= \left( \frac{r_t^2}{4R_c^2} \right) \left( \frac{R_c^3 \rho_c}{\frac{100}{x} r_t^3 \rho_t - r_t^3 \rho_t} \right) \quad (4-9)$$

$$= \left( \frac{r_t^2}{4R_c^2} \right) \left( \frac{R_c^3 \rho_c}{\left( \frac{100}{x} - 1 \right) r_t^3 \rho_t} \right) \quad (4-10)$$

$$= \left( \frac{1}{4 \left( \frac{100}{x} - 1 \right)} \right) \left( \frac{R_c \rho_c}{r_t \rho_t} \right) \quad (4-11)$$

$$\text{Coverage} = \left( \frac{x}{4(100-x)} \right) \left( \frac{R_c \rho_c}{r_t \rho_t} \right) \quad (4-12)$$

The following is an example of calculation for the toner (carbon black) coverage on the surface of the carrier (steel carrier).

Let assume that density of the carrier ( $\rho_c$ ) = 7.87 g/cc, density of the toner ( $\rho_t$ ) = 1.2 g/cc, radius of the carrier ( $R_c$ ) = 50  $\mu\text{m}$ , and radius of toner ( $r_t$ ) = 4  $\mu\text{m}$ .

Toner concentration : 1 wt%

$$\begin{aligned} \text{Coverage} &= \left( \frac{1}{4(100-1)} \right) \left( \frac{(50)(7.87)}{(4)(1.2)} \right) \\ &= 0.21 \\ &= 21\% \end{aligned}$$

The calculation of the number of toner particles coverage on a carrier particle is shown below.

Surface area of the carrier :  $4\pi R_c^2$

Area of the carrier :  $\pi r_t^2$

The number of toner particles coverage (100%) on a carrier surface.

$$\begin{aligned} \text{Number of the toner particles per each carrier} &= \frac{4\pi R_c^2}{\pi r_t^2} && (4-13) \\ &= \frac{(4)(50)^2}{(4)^2} \\ &= 624 \text{ particles} \end{aligned}$$

Table 4-2 : The relationship of the toner concentration (wt%), the coverage (%), and number of the toner particles/carrier

Toner concentration (wt%)	Coverage (%)	No. of the toner particles/carrier
0.5	10	64
1	21	132
2	42	264
3	63	392
5	108	676
7	154	960
10	228	1424

Table 4-2 shows the relationship of the toner concentration (wt%), the coverage (%), and number of the toner particles/carrier of the present system. The toner coverage is higher when the toner concentration is higher, but the q/m values are lower.

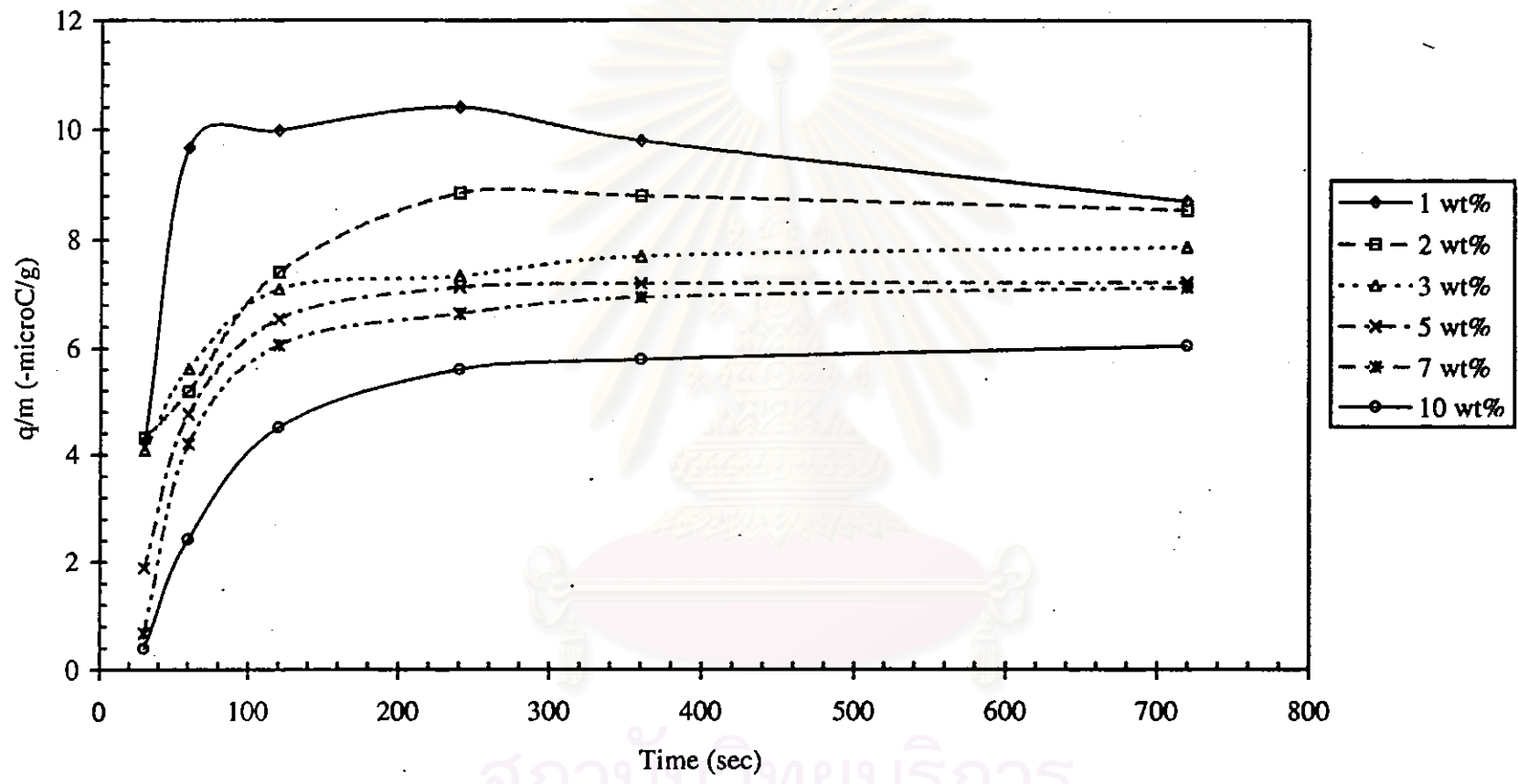


Figure 4-14 Dependence of  $q/m$  on developing time for KT-16a and F-200 at 600 rpm

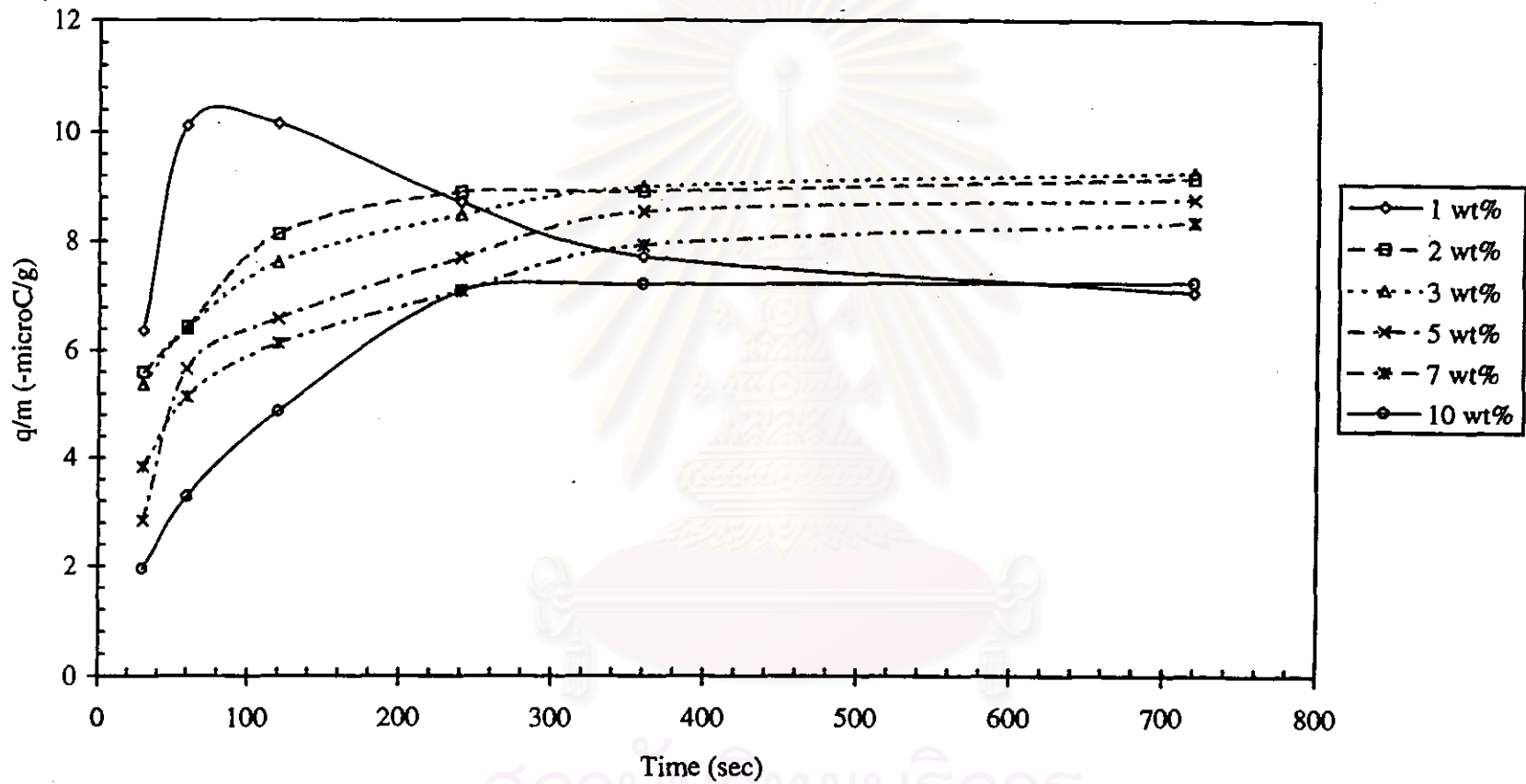


Figure 4-15 Dependence of  $q/m$  on developing time for KT-16a and F-200 at 800 rpm

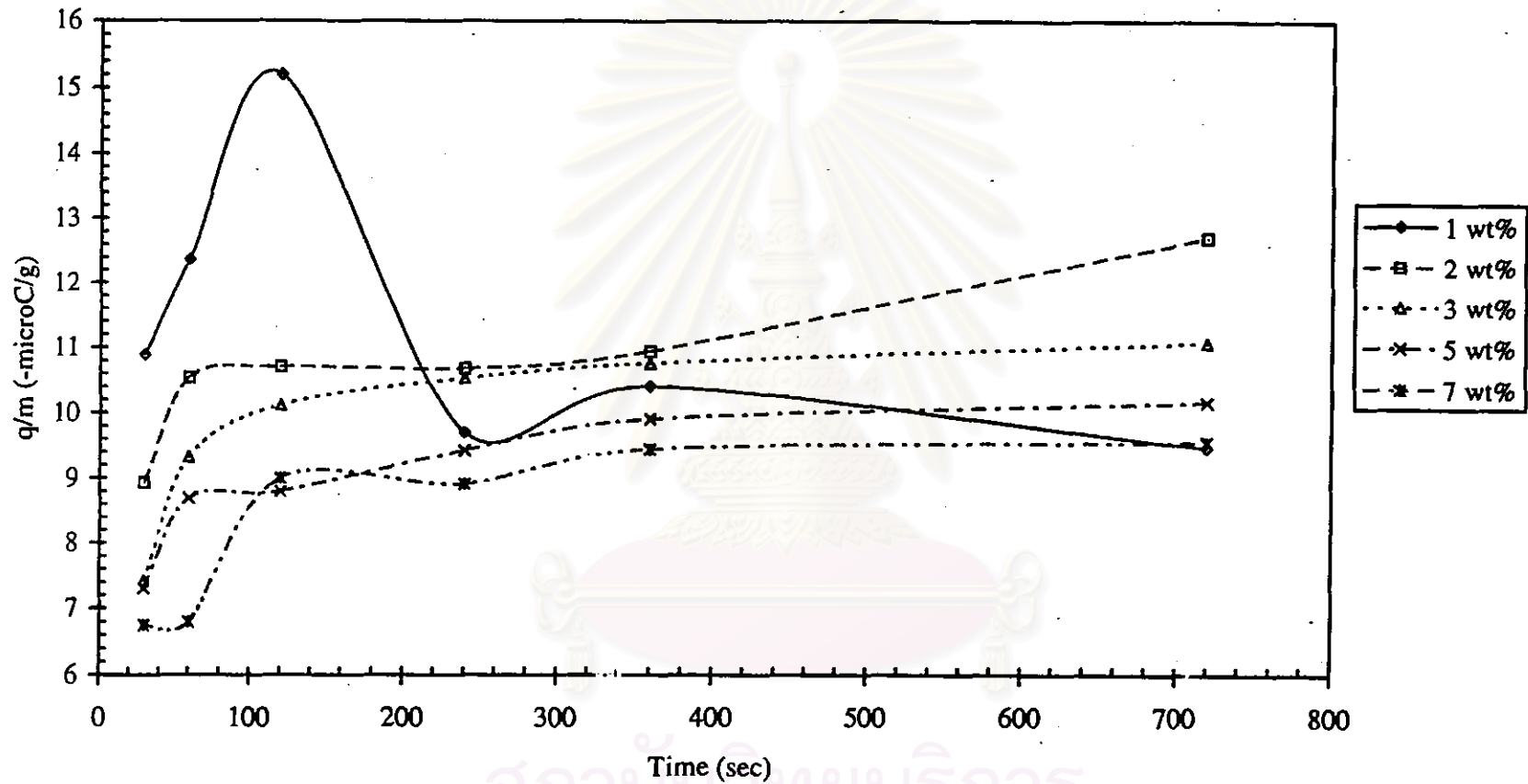
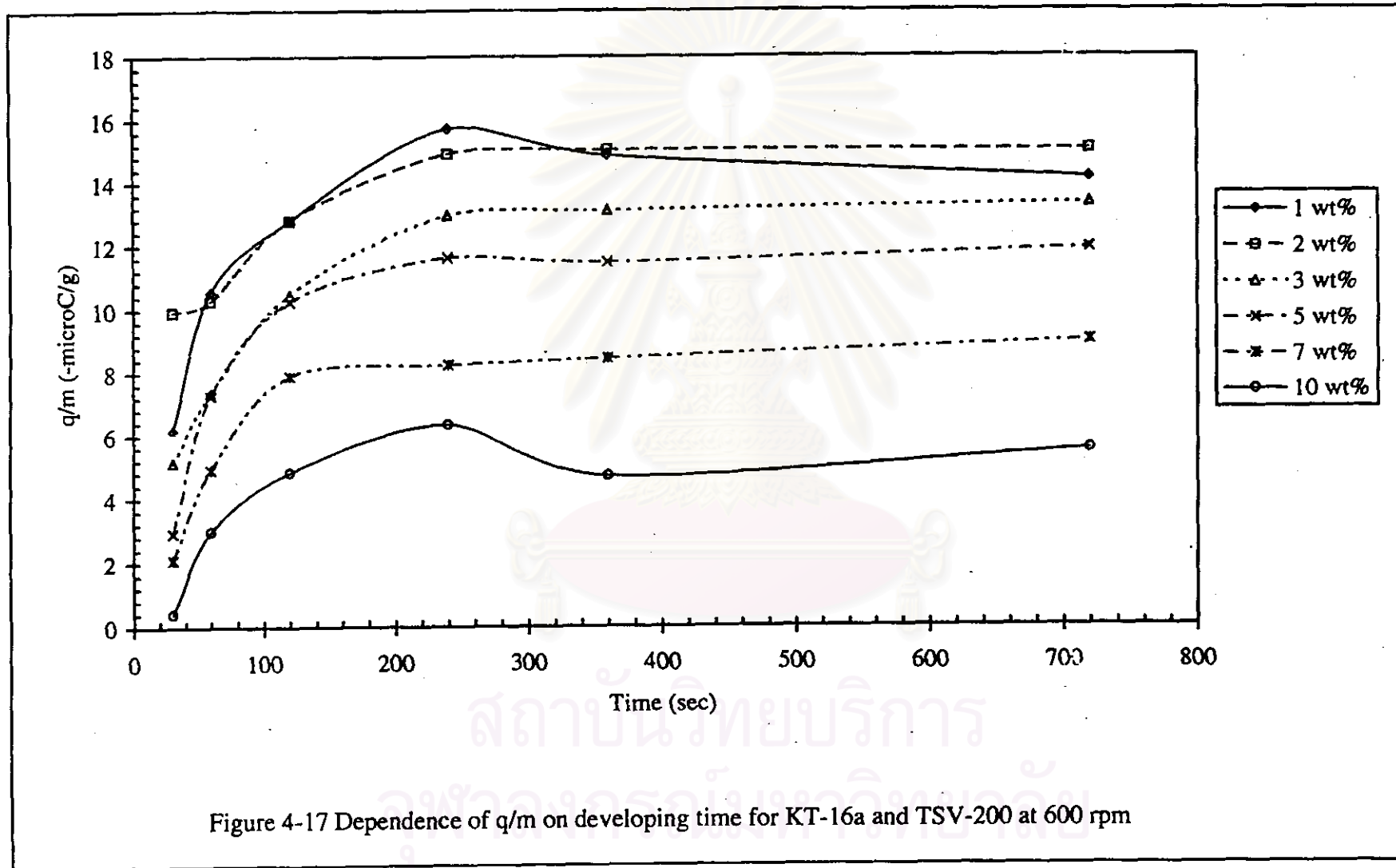


Figure 4-16 Dependence of  $q/m$  on developing time for KT-16a and F-200 at 1000 rpm





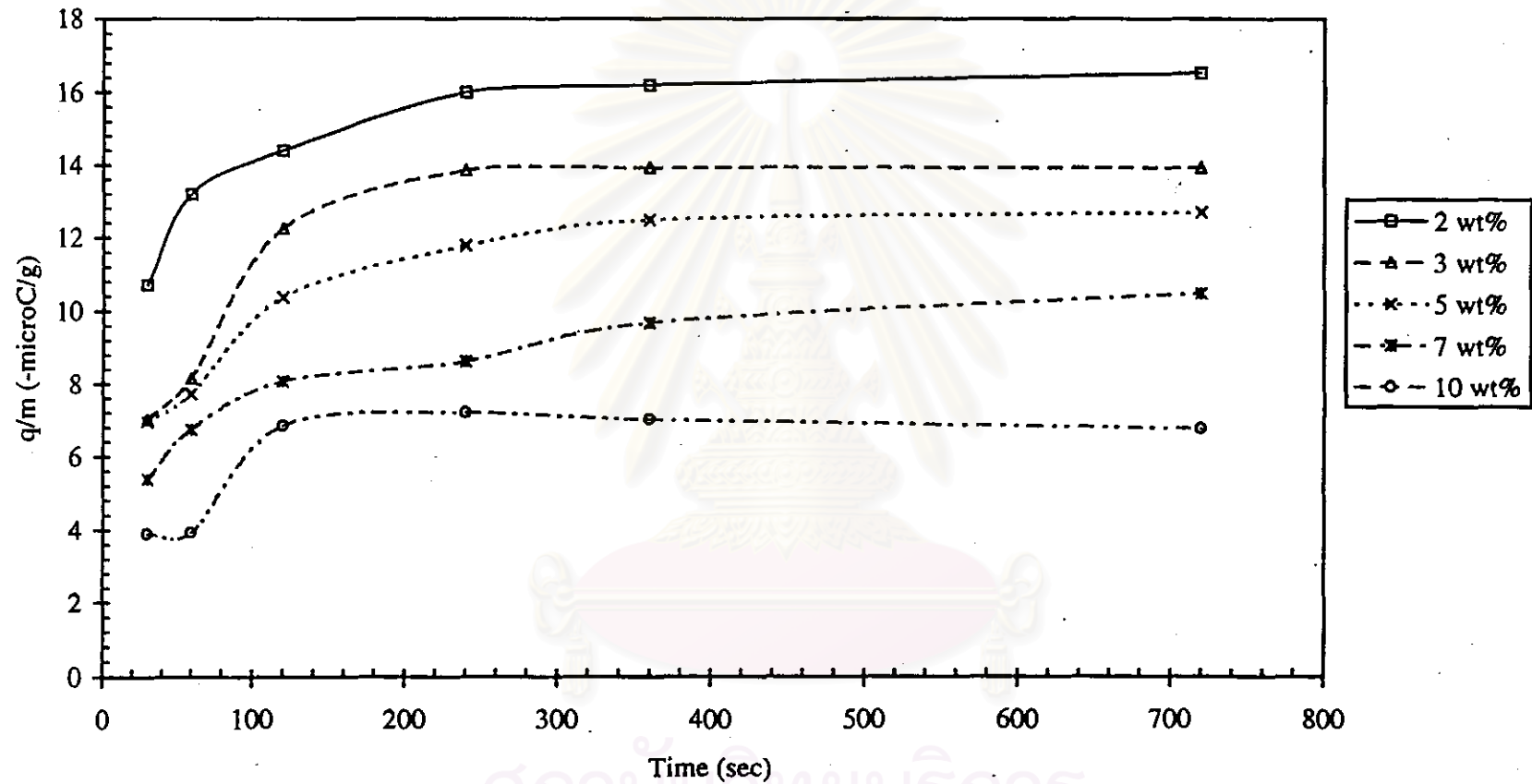


Figure 4-18 Dependence of  $q/m$  on developing time for KT-16a and TSV-200 at 800 rpm

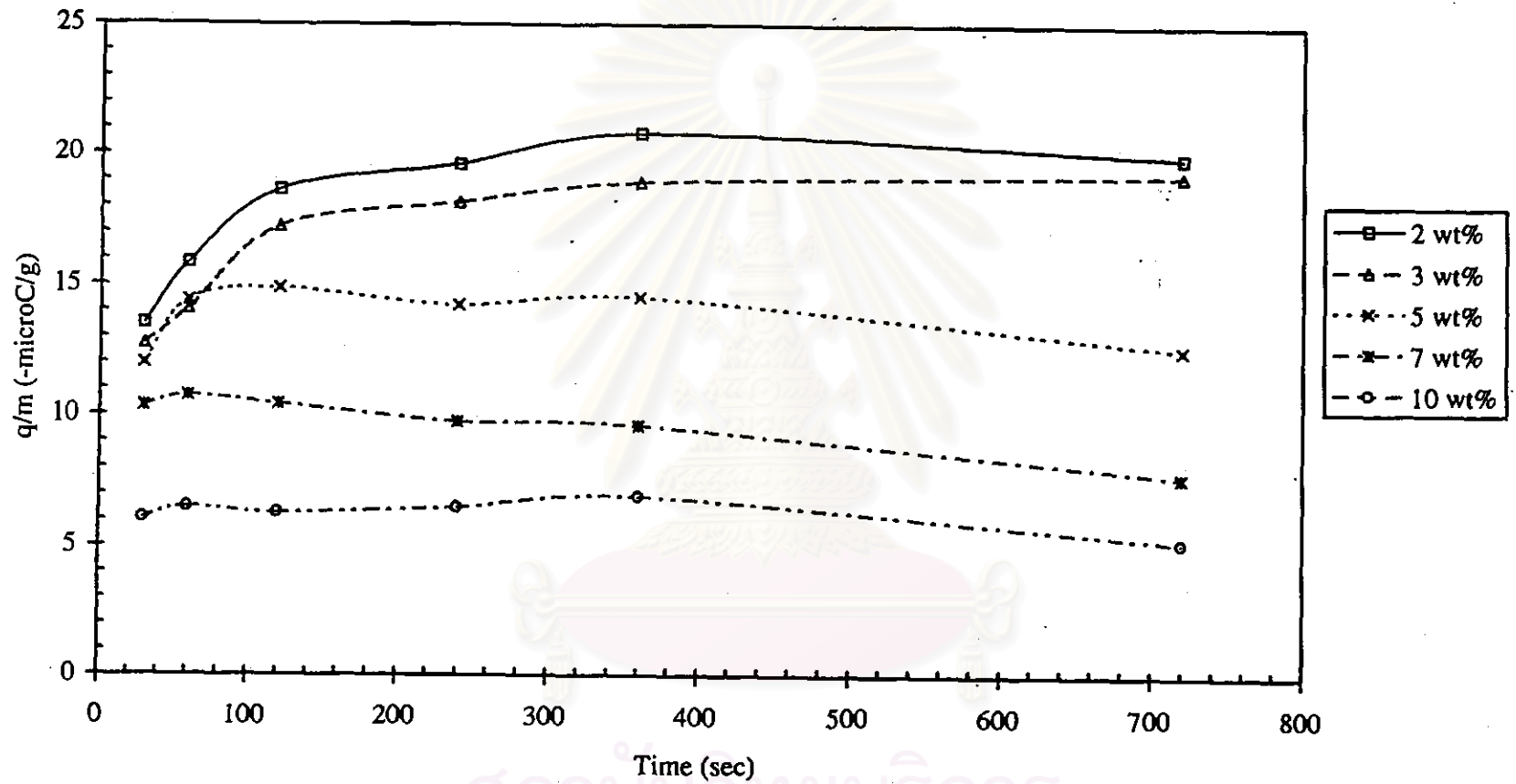


Figure 4-19 Dependence of  $q/m$  on developing time for KT-16a and TSV-200 at 1000 rpm

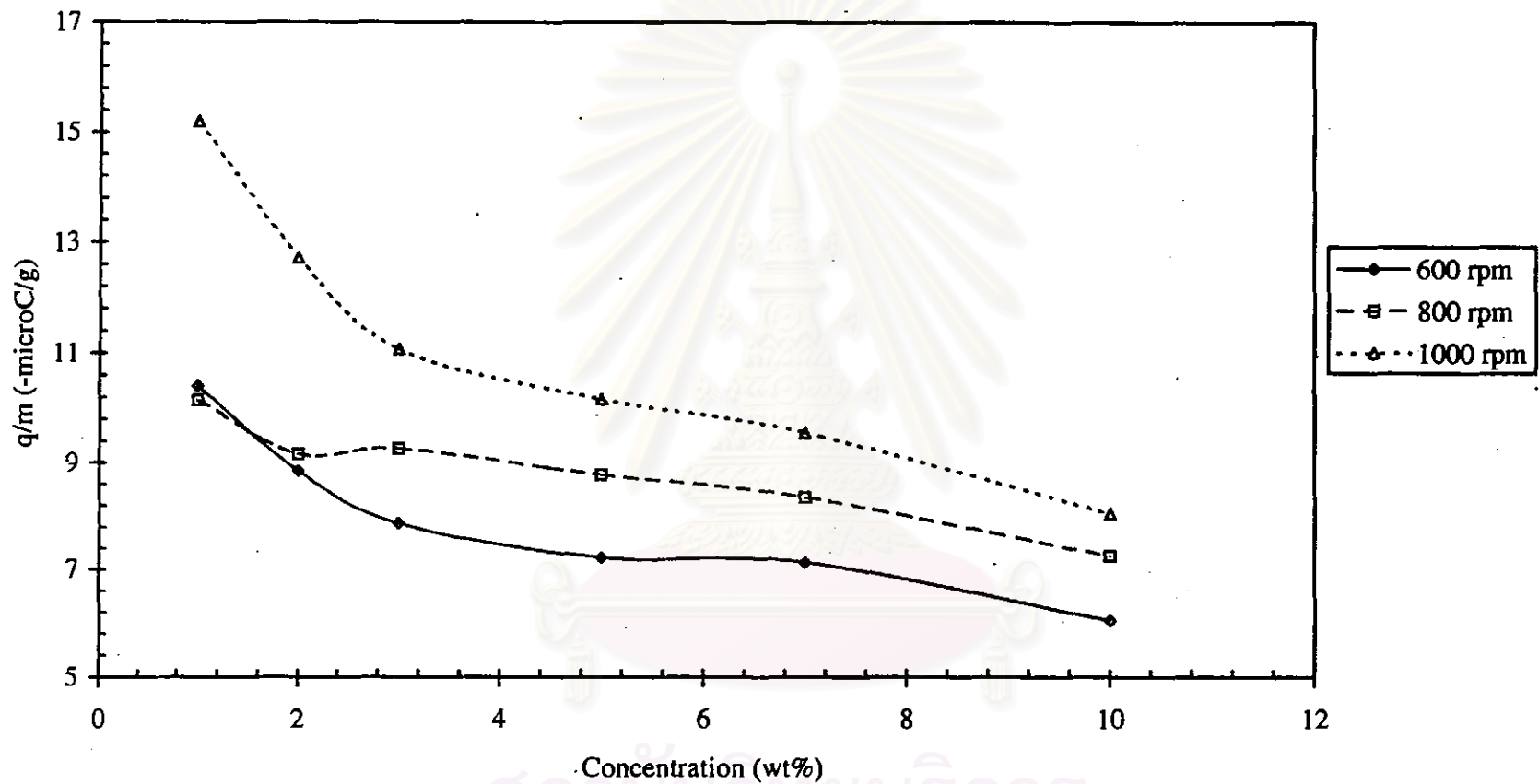


Figure 4-20 Dependence of q/m (max) on toner concentration for KT-16a and F-200

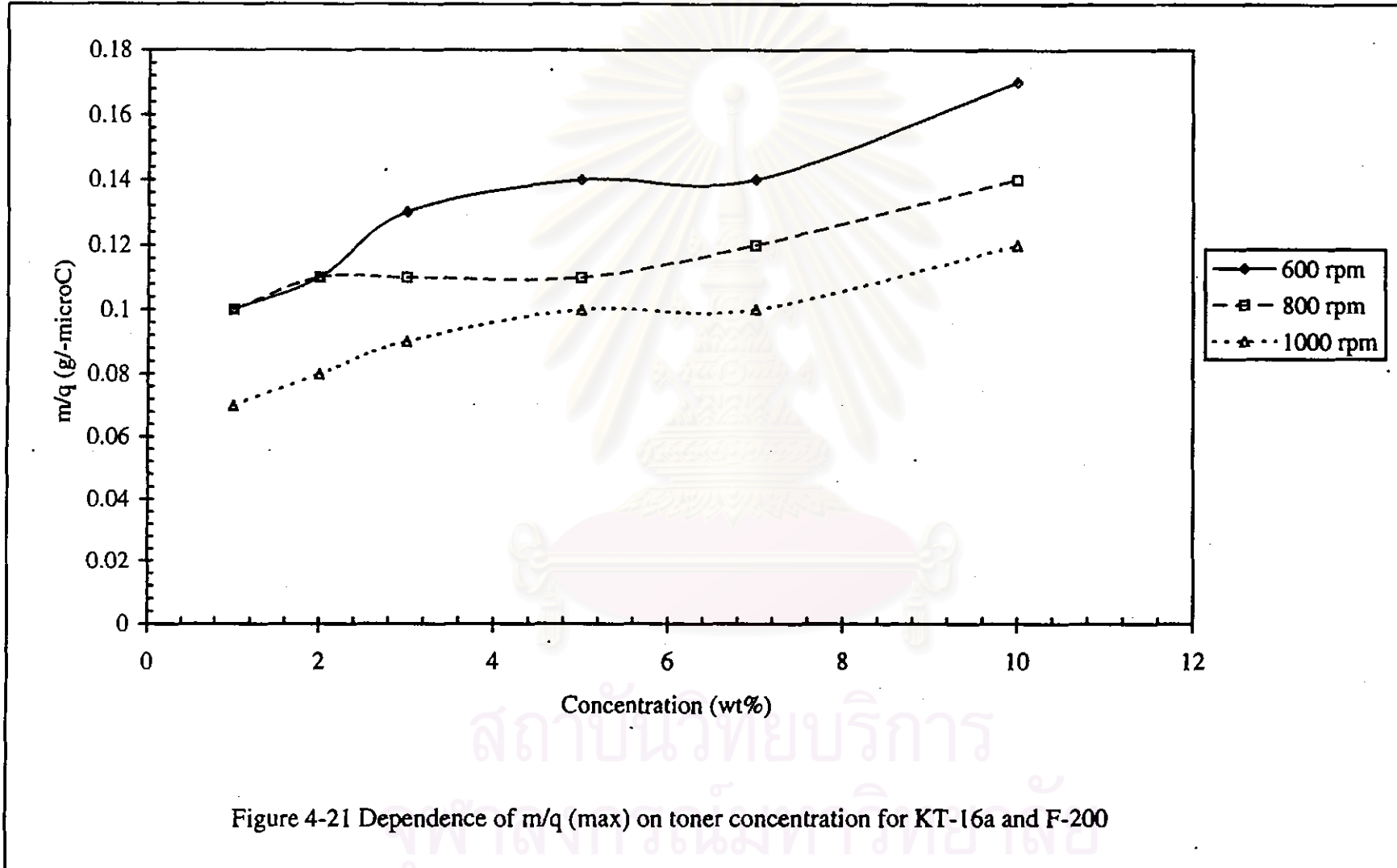


Figure 4-21 Dependence of  $m/q$  (max) on toner concentration for KT-16a and F-200

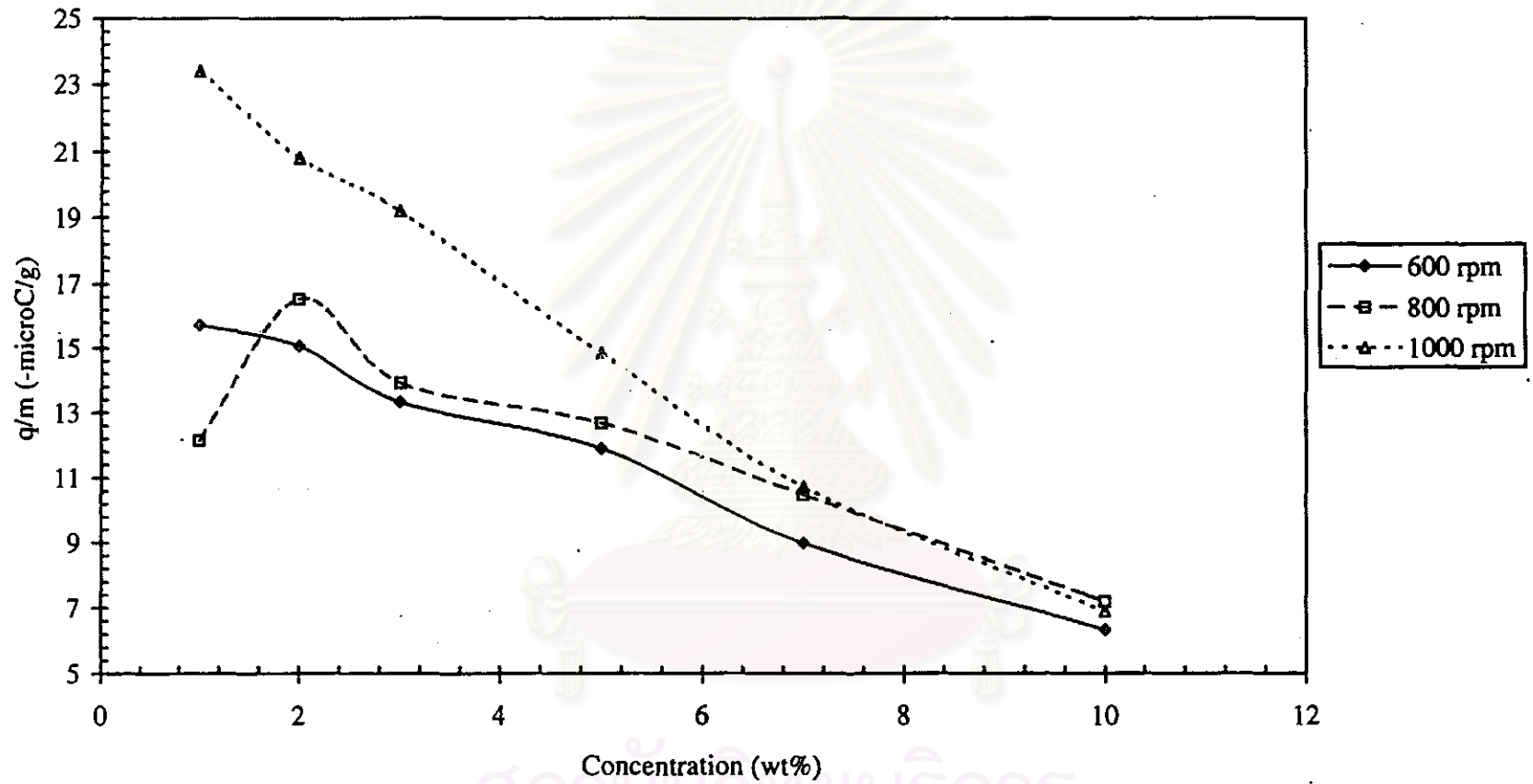


Figure 4-22 Dependence of  $q/m$  (max) on toner concentration for KT-16a and TSV-200

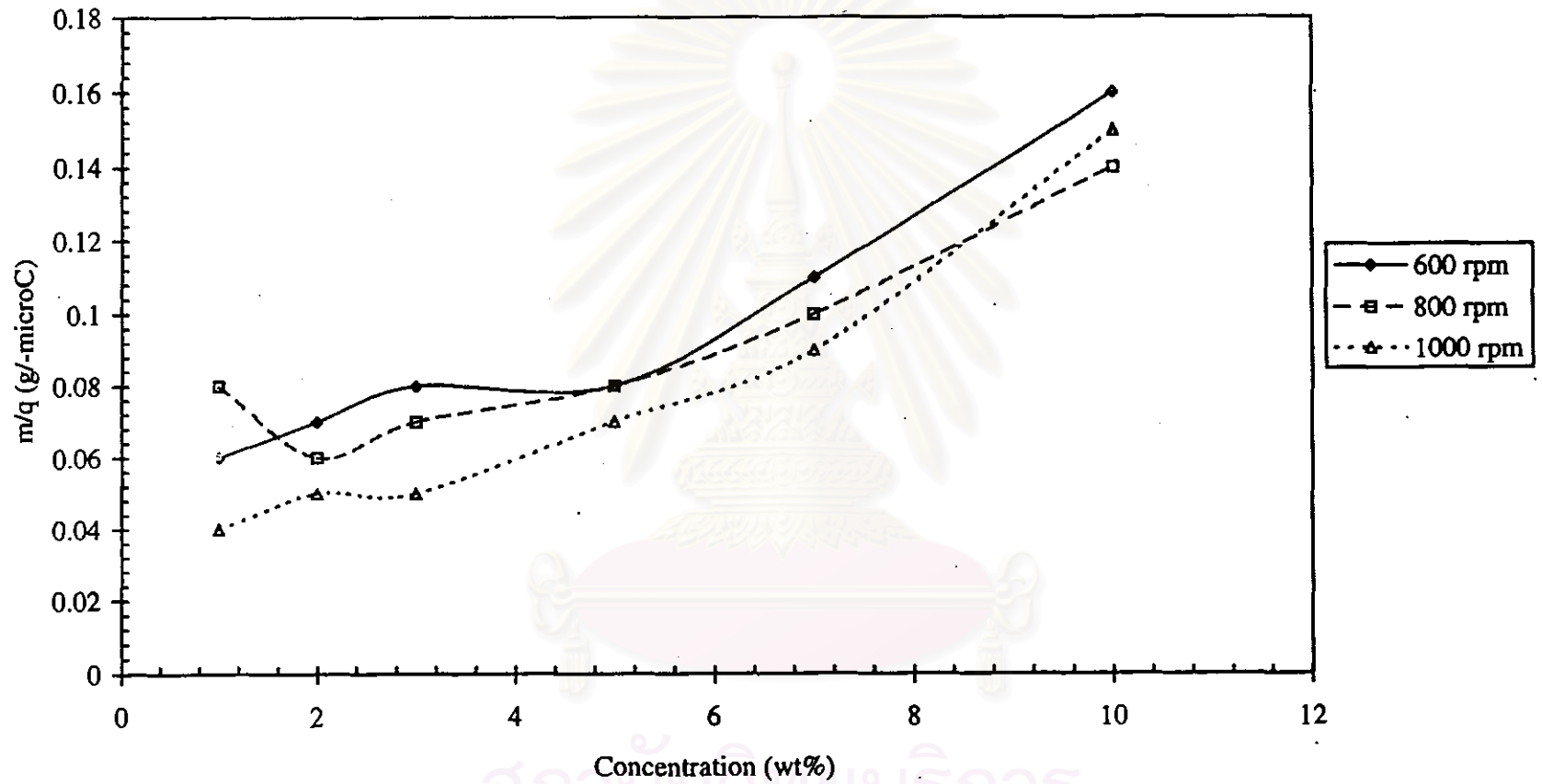


Figure 4-23 Dependence of  $m/q$  (max) on toner concentration for KT-16a and TSV-200

#### 4.5 Morphological appearance of material surfaces

The scanning electron micrographs of the developer mixed, KT-16a toner plus F-200 carrier, on the various toner concentrations of 1, 2, 3, 5, 7, and 10 wt% at the rotating speed of 800 rpm are shown in Figure 4-24. The SEM photos show that the toner coverage on a carrier increased with increasing toner concentration.

#### 4.6 Toner shape dependency

Two kinds of toners, with dissimilar shapes (irregularly-shaped toner (KT-16a) and spherical-shaped toner (N-O9S)), were mixed separately with each type of ferrite carrier (F-200) or steel carrier (TSV-200) in a rotating roller (glass cell, 24 mm in diameter). All developers were prepared for five wt% of toner at a rotating speed of 600 rpm. The tribocharge of the toner ( $q/m$ ) was then measured by a blow off measurement unit. The tribocharge of the toner was measured as a function of rotation time at 720 seconds. Figure 4-25 shows the change in the toner charge-to-mass ratio for the spherical-shaped toner, N-O9S toner, and the irregularly-shaped toner, KT-16a toner, with the same carrier, TSV-200. The N-O9S toner and the KT-16a toner were each mixed with F-200 carrier by a rotating roller. The effects of the rotating times on the  $q/m$  values are shown in Figure 4-26.

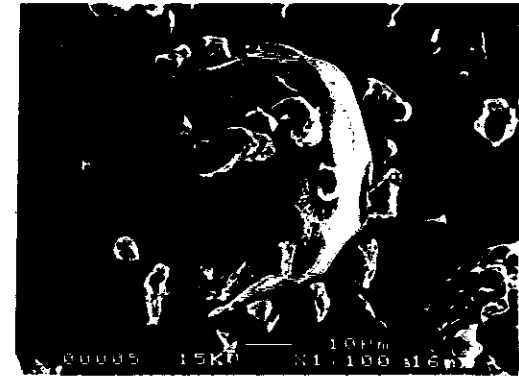
In both toners, the trends for all of the curves are similar. The  $q/m$  values were rapidly changed in 240 seconds and slightly changed until 720 seconds. These  $q/m$  values were determined by the slopes of the curves. The  $q/m$  values of the spherical-shaped toner were found to be larger than the irregularly-shaped toner at the same rotation conditions. This is due to more surface area of contact of the spherical-shaped toner. The CCA on the surface of irregularly-shaped toner does not charge the entire surface. This is because the surface is not smooth and some areas are difficult to charge. Therefore, the  $q/m$  values are less than that of the spherical-shaped toner. Another reason could be explained by the dielectric breakdown which was easy to occur in the irregular toner than in the spherical one.<sup>22</sup> On the other hand, the time constant for charging of the spherical toner was smaller than that of the irregular toner.



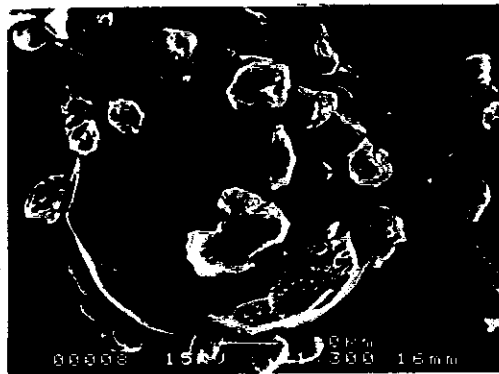
1 wt%



2 wt%



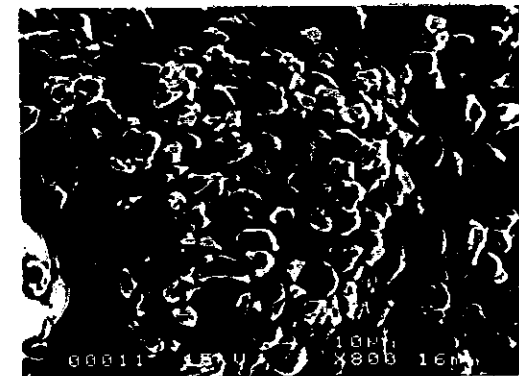
3 wt%



5 wt%



7 wt%



10 wt%

Figure 4-24 Scanning electron micrographs of the developers, KT-16a toner and F-200 carrier, with various toner concentrations of 1, 2, 3, 5, 7, and 10 wt%



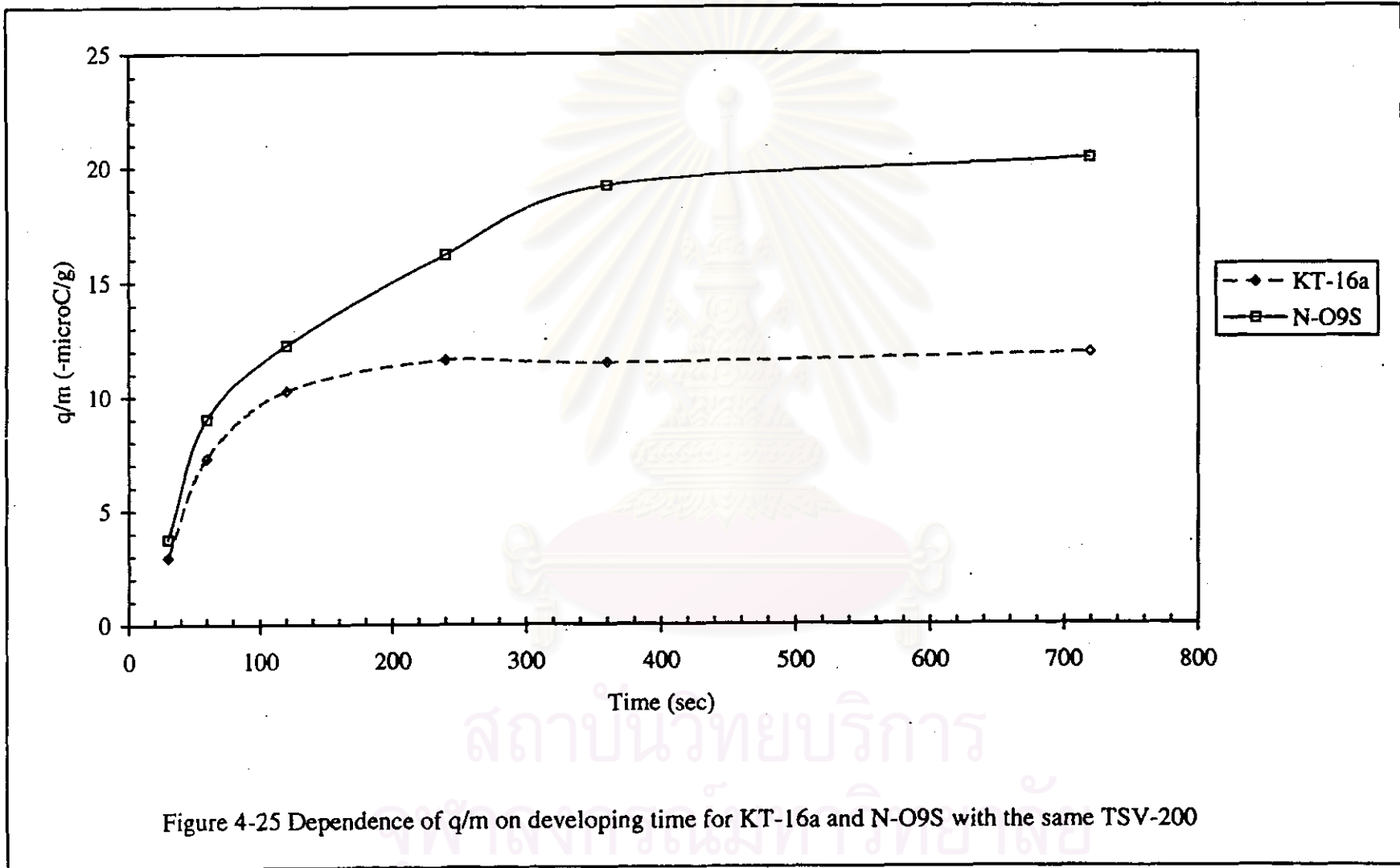


Figure 4-25 Dependence of  $q/m$  on developing time for KT-16a and N-O9S with the same TSV-200

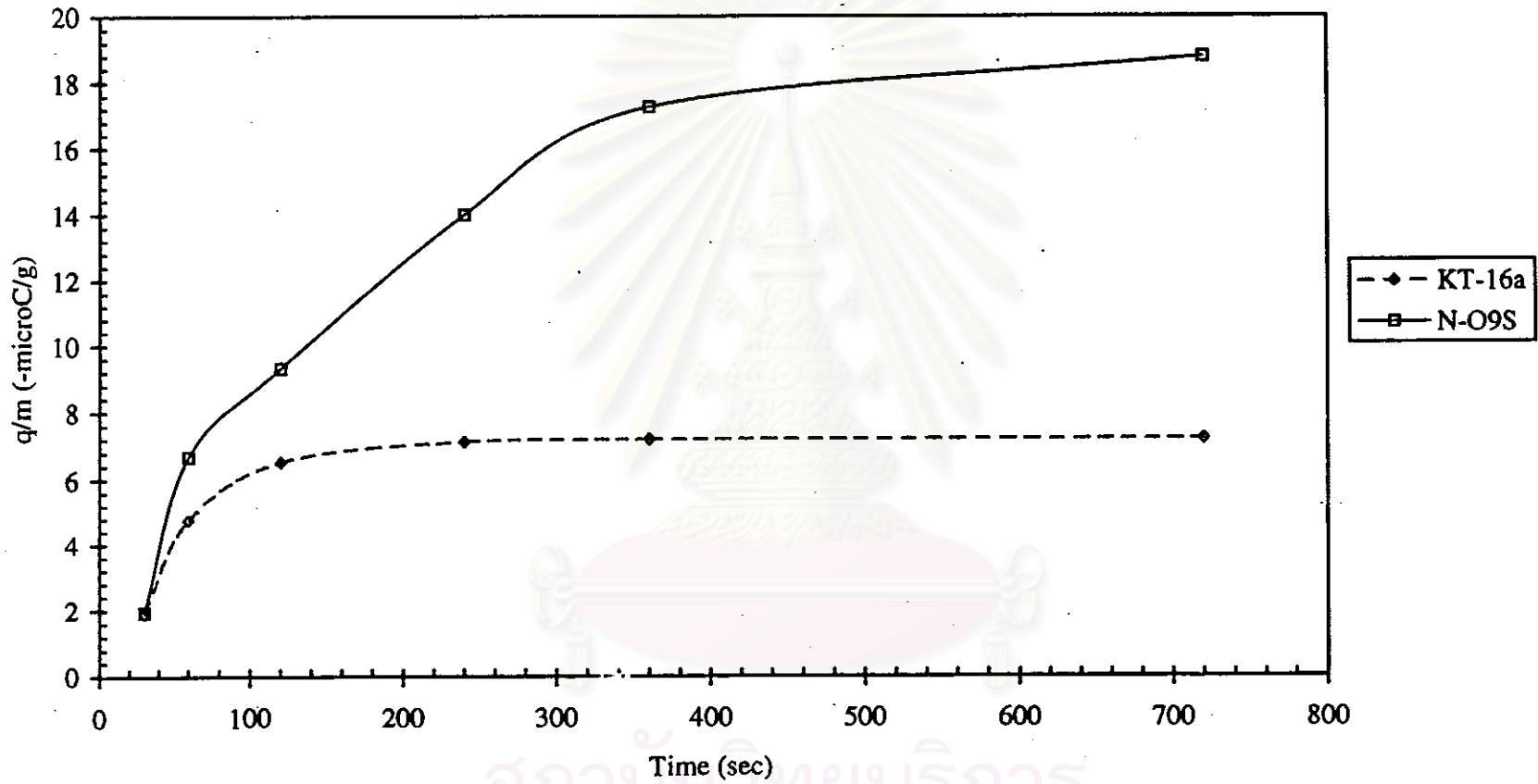


Figure 4-26 Dependence of  $q/m$  on developing time for KT-16a and N-O9S with the same F-200

#### 4.7 Carrier dependency

The irregular toner, KT-16a, and the spherical toner, N-O9S, were mixed with each type of the carriers, F-200 carrier and TSV-200 carrier, in the glass cell. The toner-to-carrier wt% ratio of two developers (one for the KT-16a toner and F-200 carrier, the other one for the KT-16a toner and TSV-200 carrier) had a value of 3 wt% with the rotating speed at 800 rpm. The toner was charged by putting into contact with the carriers. The charge-to-mass ratio ( $q/m$ ) of KT-16a toner and carrier with different components, of the ferrite carrier and the steel carrier, (Figures 4-29 and 4-30), measured by a blow off measurement unit, is shown in Figure 4-27. From Figures 4-29 and 4-30, the elemental components of the F-200 carrier are Fe, Cu, and Zn, and only Fe is found in the TSV-200 carrier. The elemental content is shown in Table 4-3. The ratios increased rapidly from zero and approached a quasistatic value that changed very slowly thereafter.

The toner concentration (wt%) from the N-O9S toner that was mixed with F-200 carrier and TSV-200 carrier had a value of 5 wt% at a rotating speed of 600 rpm. The toner charge-to-mass ratios ( $q/m$ ) for N-O9S toner and different carriers were plotted as a function of time in Figure 4-28.

As a whole, the  $q/m$  values at the equilibrium state of developers with TSV-200 carriers were more than those of the F-200 carrier, similar to that measured by Takahashi.<sup>19</sup> An explanation to this occurrence is that the steel carrier has strong tribocharging points more than ferrite carrier. This means that the TSV-200 carrier, which had only Fe in the component, gave the stronger contact with the toner. Then, the high  $q/m$  values was resulted; but the F-200 carrier gave almost the constant  $q/m$  values, which were smaller than the  $q/m$  values of the steel carrier. The range of  $q/m$  values of the two developers, KT-16a toner mixed with F-200 carrier or TSV-200 carrier, were larger than that of the developers of N-O9S toner with the same carrier. These  $q/m$  values were determined by the characteristics of the curves. It can be concluded that the charge characteristics of the toner in a two-component developer depend on the surface properties of the carrier.

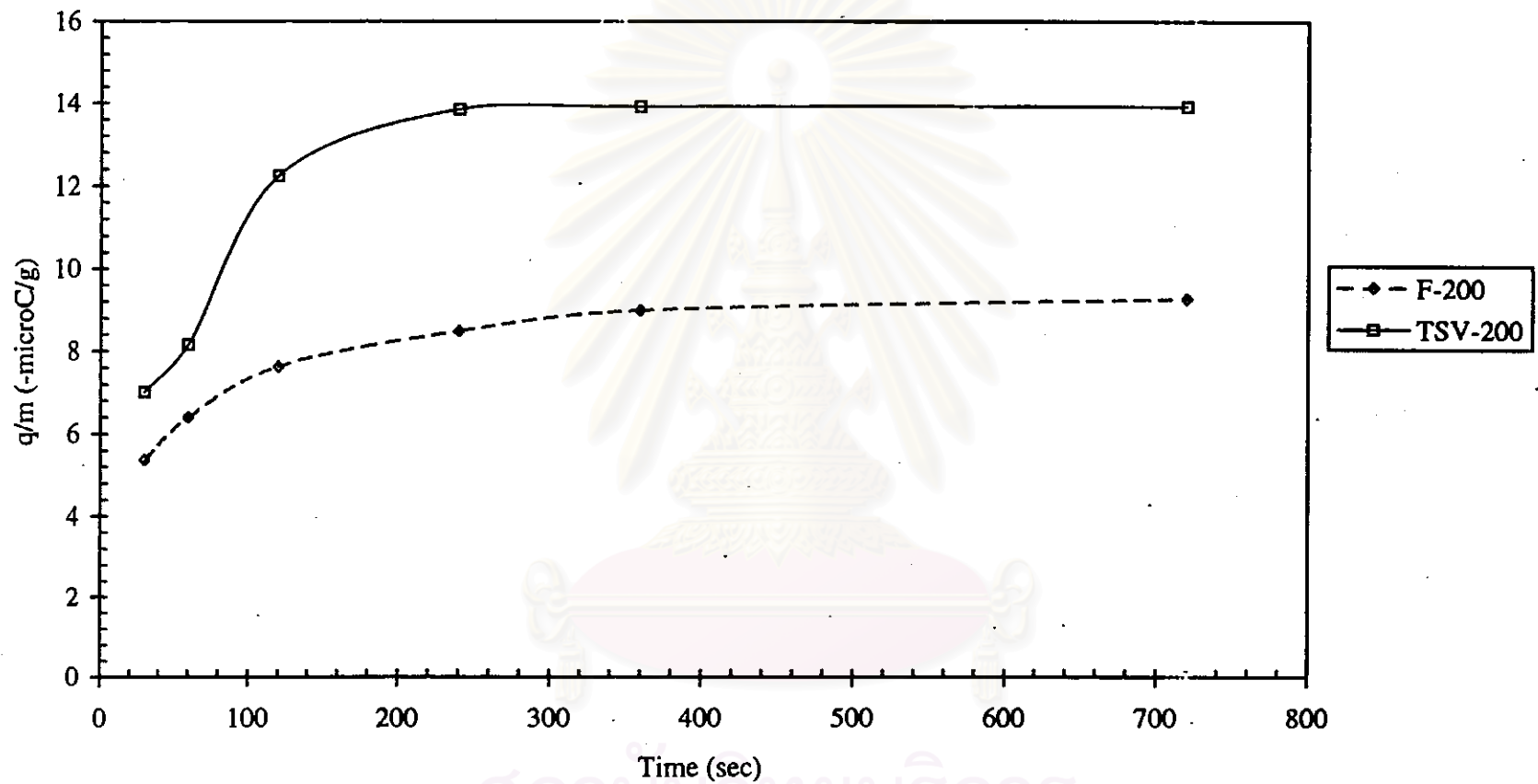


Figure 4-27 Dependence of  $q/m$  on developing time for KT-16a with F-200 and TSV-200

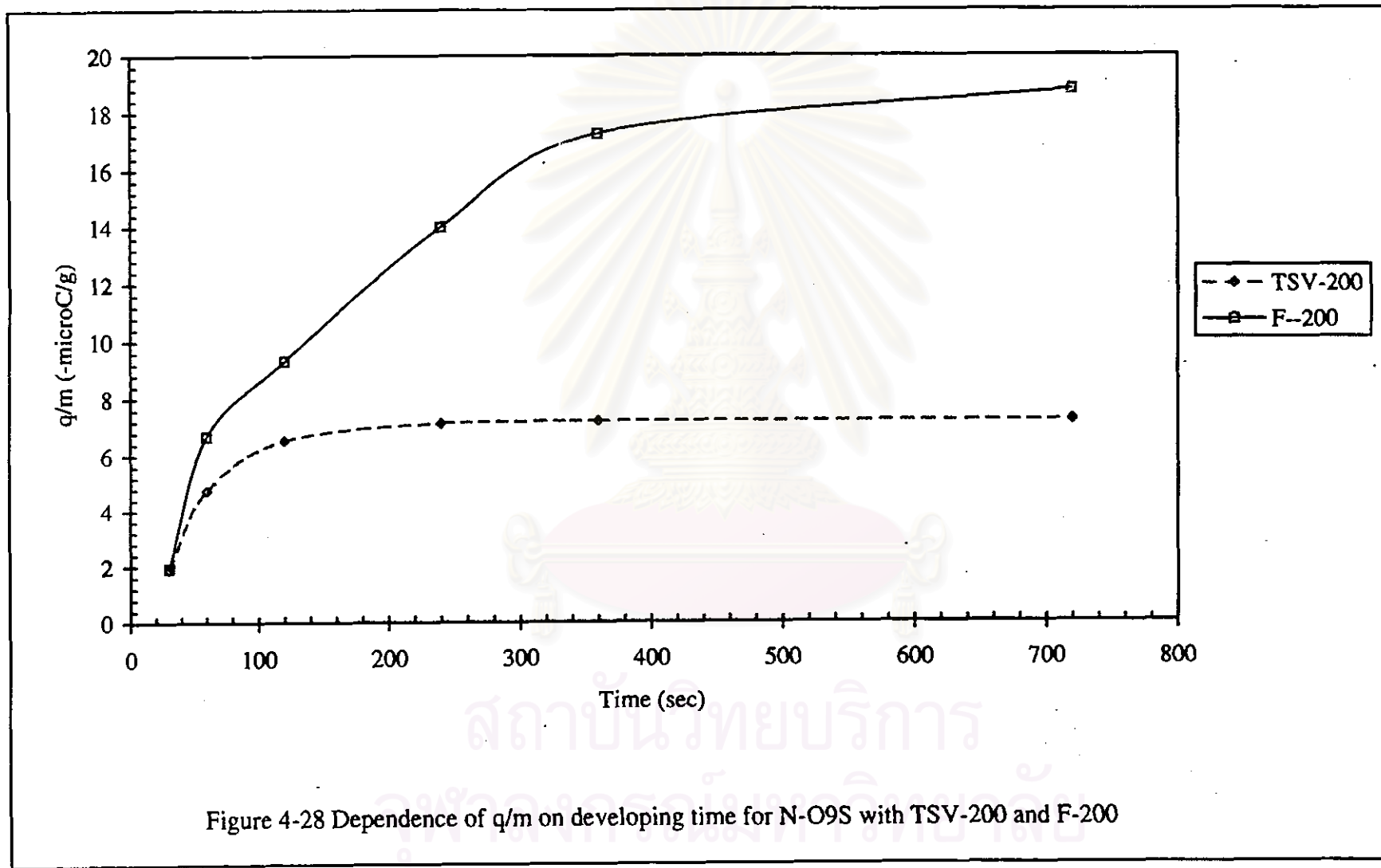


Figure 4-28 Dependence of  $q/m$  on developing time for N-O9S with TSV-200 and F-200

JEOL JED-2140  
QUANTITATIVE ANALYSIS vers. 1.0

Sample name : F200-HT 15 kV  
Measurement date : 1999/2/13 14:24:51

-----Geometry Parameter-----

Acceleration voltage : 15 kV Coming-out angle : 30.00  
Passing time : 100.00 sec. Effective time : 74.69 sec.

-----Analysis Research-----

Element (keV)	Weight (%)	Error	Atomic no.(%)	Compound Weight (%)	K Ratio
C_K	0.28	18.50	0.61	39.94	0.0464
O_K	0.52	30.74	0.39	33.61	0.0506
Fe_L	0.70	32.57	0.91	15.10	0.0852
Cu_L	0.93	13.46	0.46	5.49	0.0235
Zn_L	1.01	14.78	0.50	5.86	0.0189
Total	100.00		100.00		

LIN 2K COUNT

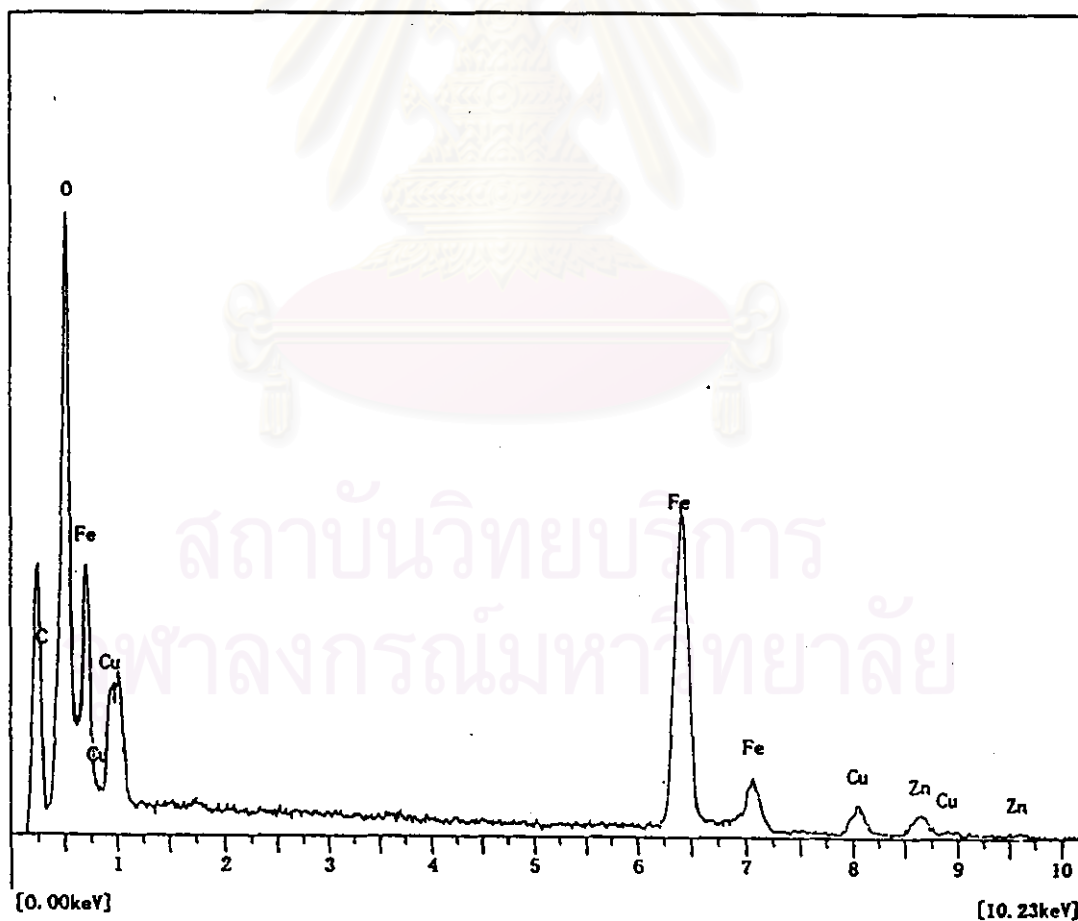


Figure 4-29 Elemental analysis of F-200 carrier

JEOL JED-2140  
QUANTITATIVE ANALYSIS vers. 1.0

Sample name : TSV200-HT 15 kV  
Measurement date : 1999/2/13 14:59:34

-----Geometry Parameter-----

Acceleration voltage : 15 kV Coming-out angle : 30.00  
Passing time : 100.00 sec. Effective time : 75.53 sec.

-----Analysis Research-----

Element	(keV)	Weight (%)	Error	Atomic no.(%)	Compound	Weight (%)	K Ratio
C_K	0.28	55.68	0.65	74.40			0.2827
O_K	0.52	17.98	0.41	18.03			0.0284
Fe_L	0.70	26.34	0.91	7.57			0.0768
Total		100.00		100.00			

LIN 2K COUNT

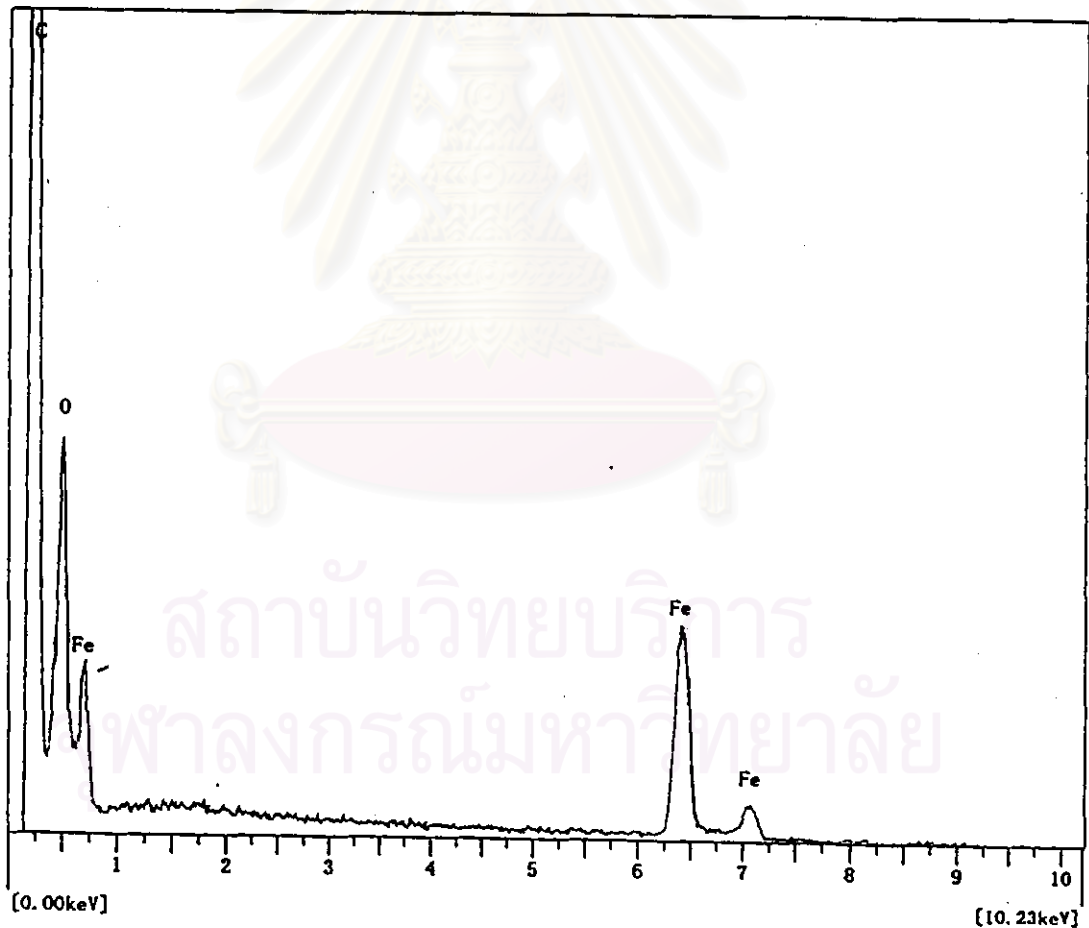


Figure 4-30 Elemental analysis of TSV-200 carrier

Table 4-3 : Elemental analysis of the carriers

Carrier Element (wt%)	TSV-200	F-200
C	55.68	18.50
O	17.98	20.74
Fe	26.34	32.52
Cu	-	13.46
Zn	-	14.78
Total	100	100

#### 4.8 Toner charge dependence on the surface layer of carrier

The toner KT-16a, was mixed with the TSV-200 carrier with currents ( $\mu\text{A}$ ) of 17, 31, 76, and 182  $\mu\text{A}$ , in its components. The toner-to-carrier wt% ratio was 5 wt% at the rotating speed of 600 rpm. Tribocharge ( $q/m$ ) of the toners was measured as a function of the rotation time at 720 seconds by the blow off method as shown in Figure 4-31. The  $q/m$  values of all of the developers were raised and reached an equilibrium state in 240 seconds. At the equilibrium state, the  $q/m$  values were in a sequential order as follows : TSV-200 (182  $\mu\text{A}$ ) > TSV-200 (76  $\mu\text{A}$ ) > TSV-200 (31  $\mu\text{A}$ ) > TSV-200 (17  $\mu\text{A}$ ). This result suggests that the current of the surface carrier affects the toner charge-to-mass ratio. This may be due to the fact that the carrier with a higher current in its component, its surface is thin. Therefore, a strong charging occurs when the toner comes into contact with the surface of the carrier.



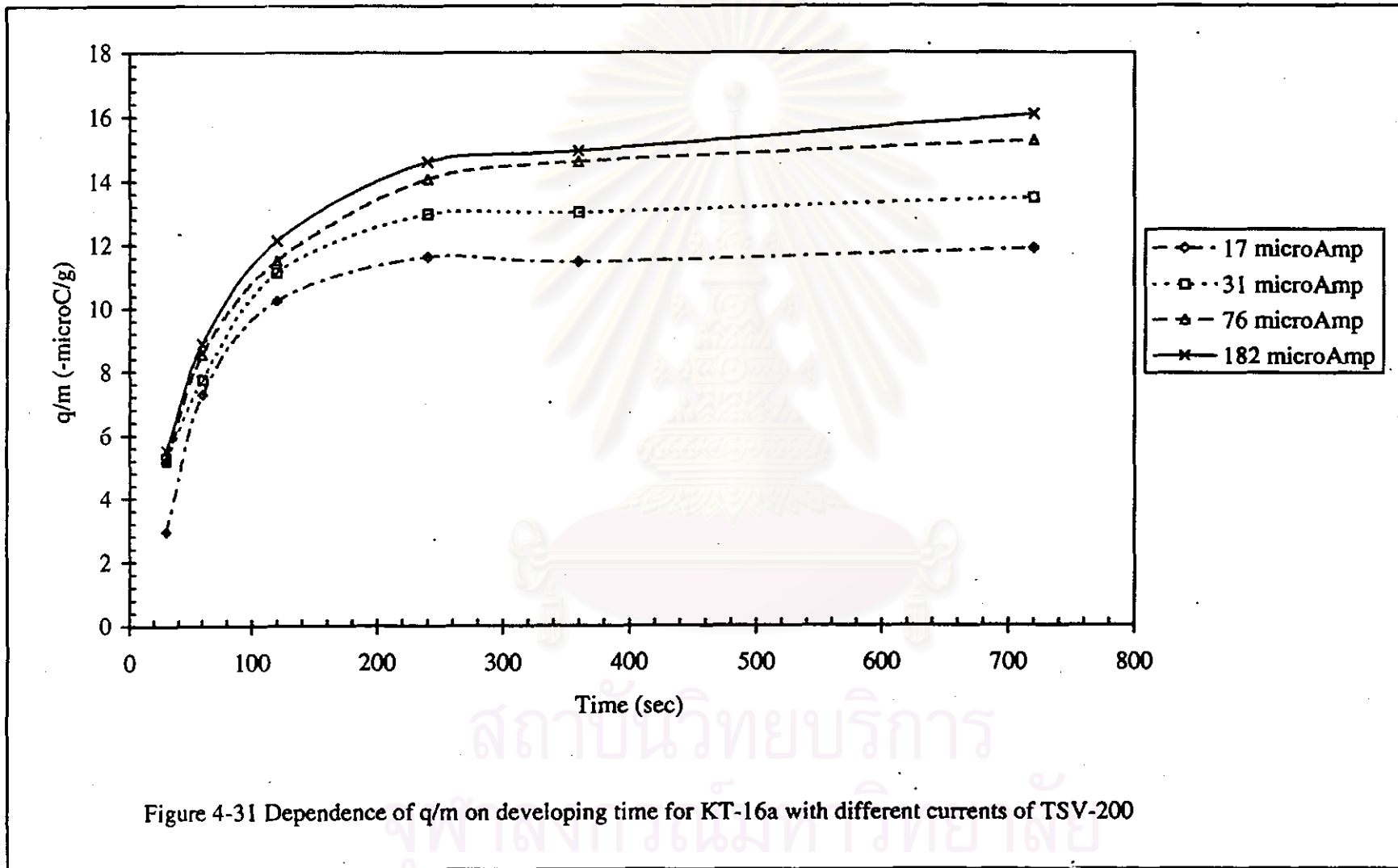


Figure 4-31 Dependence of  $q/m$  on developing time for KT-16a with different currents of TSV-200

#### 4.9 Q/m values of the toners charged by the OKI Printer

The toners, KT-16a and N-O9S, were chosen to measure their charge properties at the three conditions, which are before transferring to the photoconductor (PC), on the PC, and after transferring to the PC. These measurements were taken by the exposures (%) of 100, 60, 40, and 0 on the PC by the Blow-off method. Figure 4-32 shows a model of toner transferring to the PC by electric force. The comparison of q/m values between the KT-16a toner and N-O9S toner is shown in Table 4-4.

Table 4-4 : q/m values between the KT-16a toner and the N-O9S toner under the condition of the OKI printer

Exposure (%)	Measurement (transfer to PC)	Q/M (- $\mu$ C/g)	
		KT-16a	N-O9S
100%	Before	13.00	31.47
	On PC	16.43	36.93
	After	-	34.00
60%	Before	11.60	26.90
	On PC	16.95	30.30
	After	-	33.60
40%	Before	12.37	27.27
	On PC	11.88	32.70
	After	16.67	25.63
none	Before	17.43	25.10
	On PC	-	-
	After	18.57	24.30

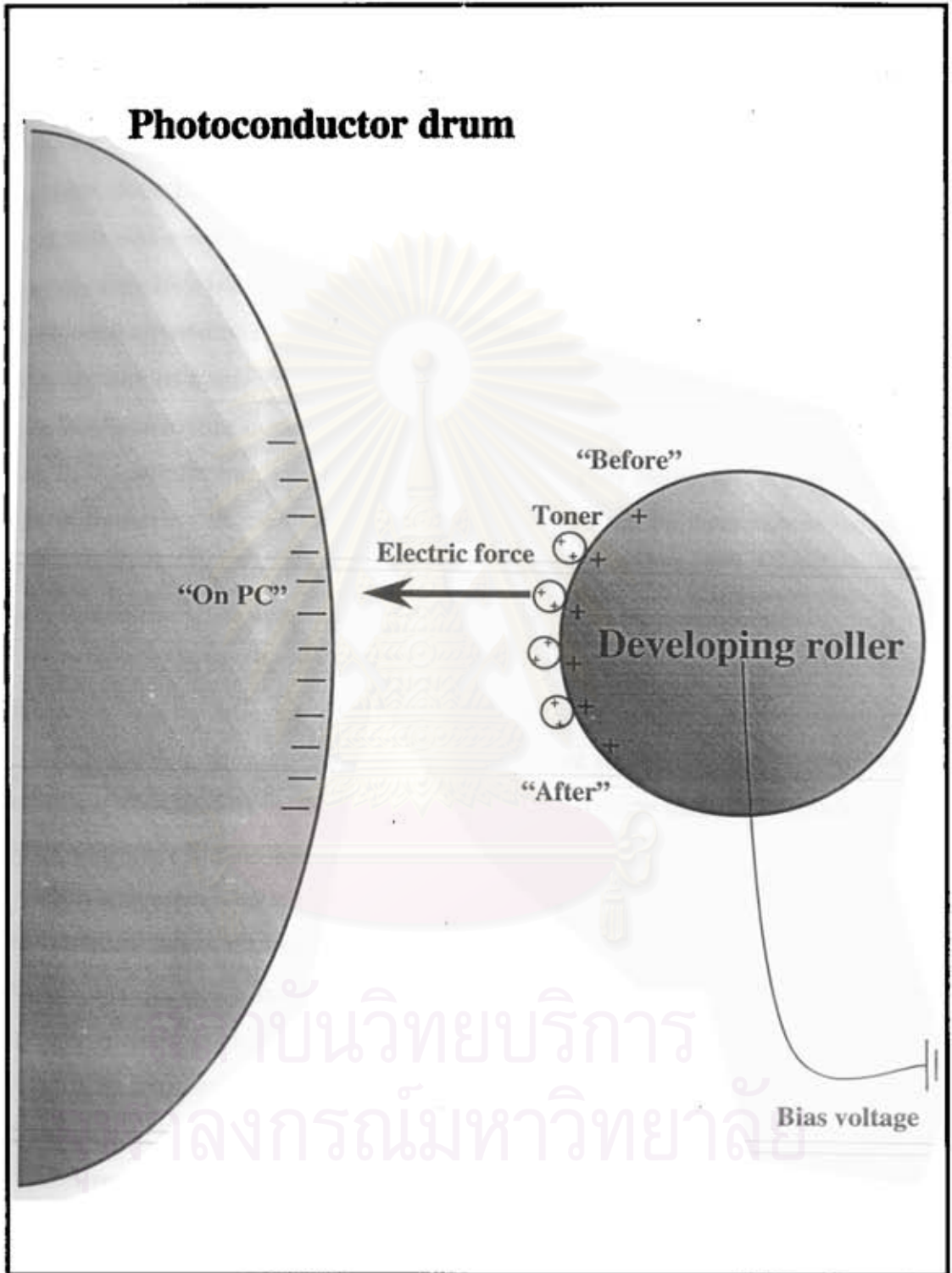


Figure 4-32 A model of toner transferring by electric force

For the KT-16a toner, the  $q/m$  at the position of "After transferring to the PC", at 100 and 60% exposure, could not be measured. This is because most of the toners were transferred onto the PC surface by both electric force ( $F_E$ ) and friction force; the charge of the toners was then very small. The  $q/m$  values "On the PC" of these exposures were higher than that of the position of "Before transferring to the PC". This result was caused by the above mentioned forces that had influenced a change in the  $q/m$  value. Exposure at 40% resulted in the electric force being reduced along with the reducing exposure. Therefore, the  $q/m$  value of "On the PC" was less than the  $q/m$  value of "Before transferring the toner to the PC". After transferring to the PC, the  $q/m$  value was higher due to the effect of the increasing electric force ( $F_E$ ). For the non-exposed case (no light irradiation on PC), the  $q/m$  values of the two positions, before transferring to the PC and after transferring to the PC, were close value and were also caused by the electric force ( $F_E$ ). The  $q/m$  value at the position "On PC" was not calculated, because there was no exposure on the PC.

For the N-O9S toner, the  $q/m$  values of 100, 60, and 40% exposure on the position of "On the PC" were more than the positions of "Before transferring to the PC". These results showed that all of the toners were moved to the PC drum, which were due to the two forces, the electric force and the friction force. The results for the non-exposed case were the same as the KT-16a toner.

In conclusion, the  $q/m$  values of the N-O9S toner were higher than the KT-16a toner at all of points of measurement. The spherical-shaped toner, N-O9S, had more efficient tribocharging than that of the irregularly-shaped toner, KT-16a. At 100% exposure on the position of "On PC", the electric force and the friction force were very strong that they could be transferred to the PC drum. So, the  $q/m$  value was higher than the other exposures. According to the 100 and 60% exposure, the position of "After transferring to the PC" could be measured only in the N-O9S toner because the N-O9S toner was a spherical-shaped toner, which had an equally nearly charging ability in each particle.

This is test form

This is test form

This is test form

ABCDEFGHIJKLMNOPQRSTUVWXYZ

abcdefghijklmnopqrstuvwxyz

1234567890



20%



40%



60%



100%



0.5 pt



1 pt



2 pt



4 pt



8 pt



16 pt

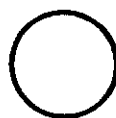
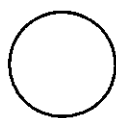
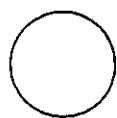


Figure 4-33 Test form

#### 4.10 Analysis of Print Quality

The toners, KT-16a and N-O9S, were selected for measuring their print qualities on uncoated paper by OKI 400 micro line CL Printer. Fifteen print-outs were printed for each type of the toners with a test form in Figure 4-33. The solid density, densities at 60 and 40% halftones, and background density of the print-outs were measured by a reflection densitometer. Figure 4-34 shows the curves of maximum density in relation to the print-outs (the copy number) of the KT-16a toner and N-O9S toner. The solid density of the two toners had little variation for all of the print-outs with a similar value (1.48).

Figures 4-35 and 4-36 show the curves of densities for 60 and 40% halftones in relation to the print-outs (the copy number) of the KT-16a toner and the N-O9S toner, respectively. The density value of each copy was almost constant, but the density values of the N-O9S toner print outs were higher than those of the KT-16a toner printed ones. The values of the print outs at 40% halftone equal to 0.70 (polymerized toner) and 0.51 (crushed toner). Likewise, the densities of the print outs for N-O9S are higher than those of KT-16a regardless of the number of copies.

The background density, measured at the non-printing area, of the N-O9S toner (0.03) and the KT-16a toner (0.02) were close value, as shown in Figure 4-37.

The edge sharpness and edge raggedness of the lines (0.5 points) and the characters of the KT-16a toner and the N-O9S toner by image analyzer are shown in Figures 4-38 to 4-49, respectively.

สถาบันวิทยบริการ  
จุฬาลงกรณ์มหาวิทยาลัย

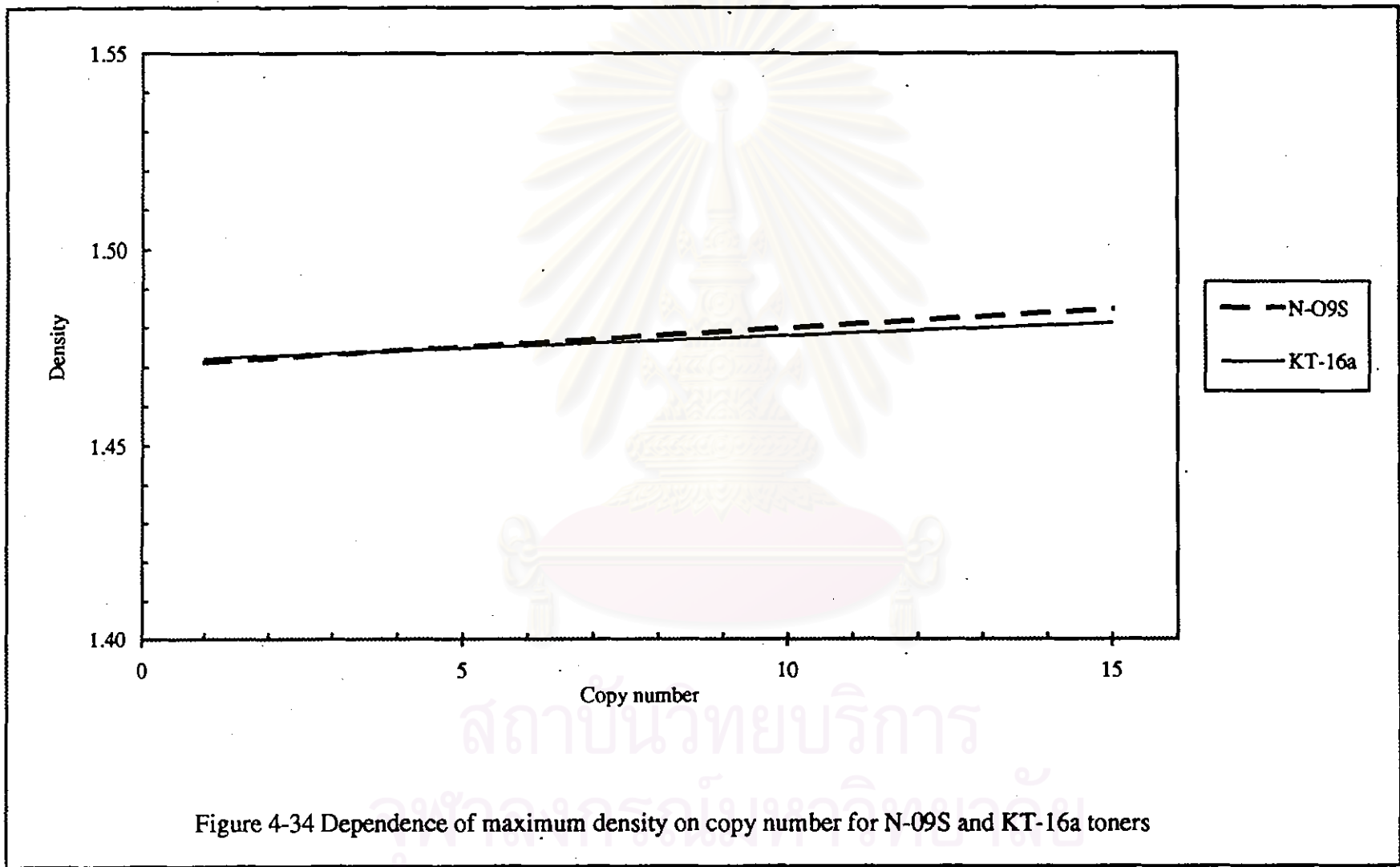
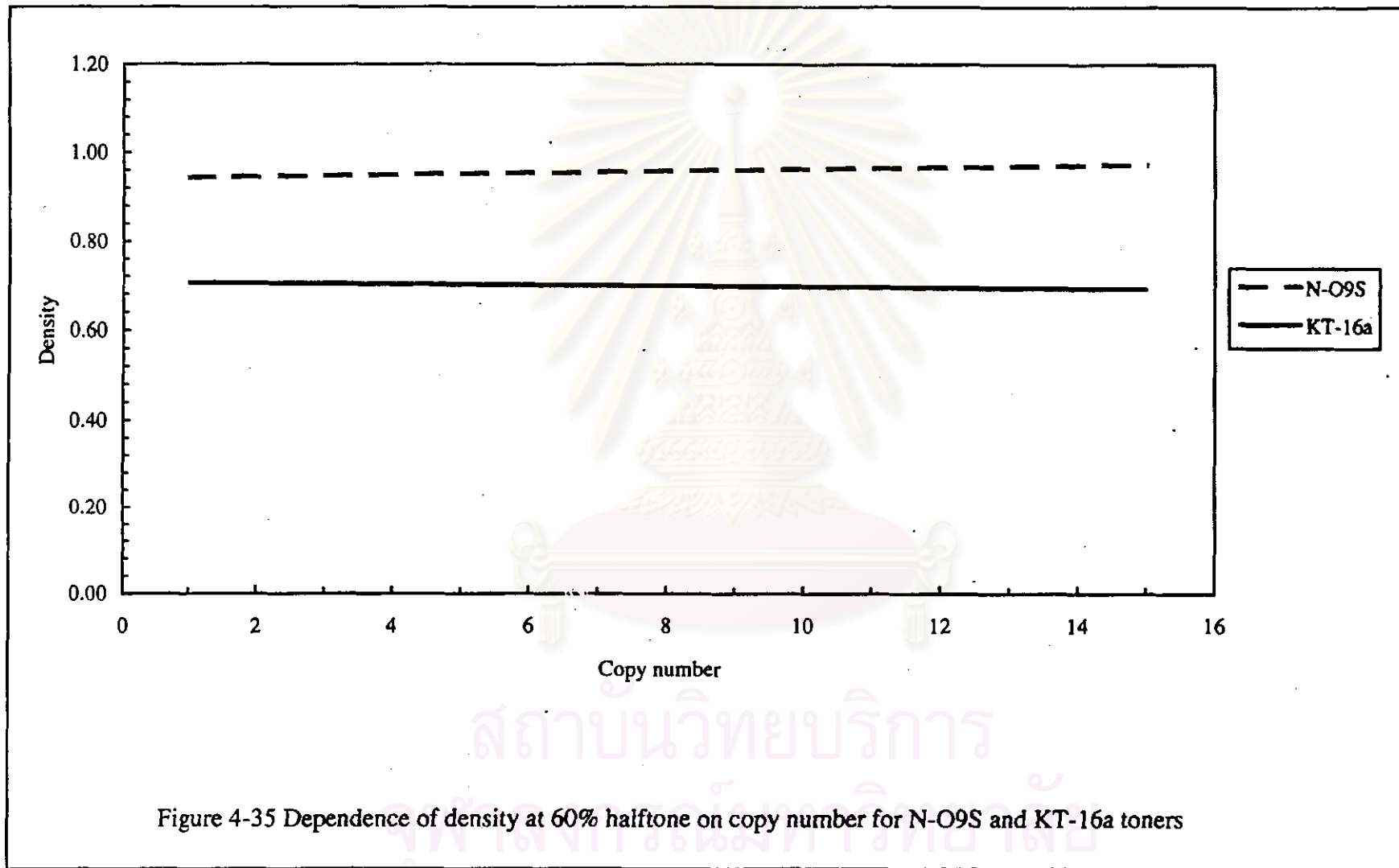


Figure 4-34 Dependence of maximum density on copy number for N-09S and KT-16a toners





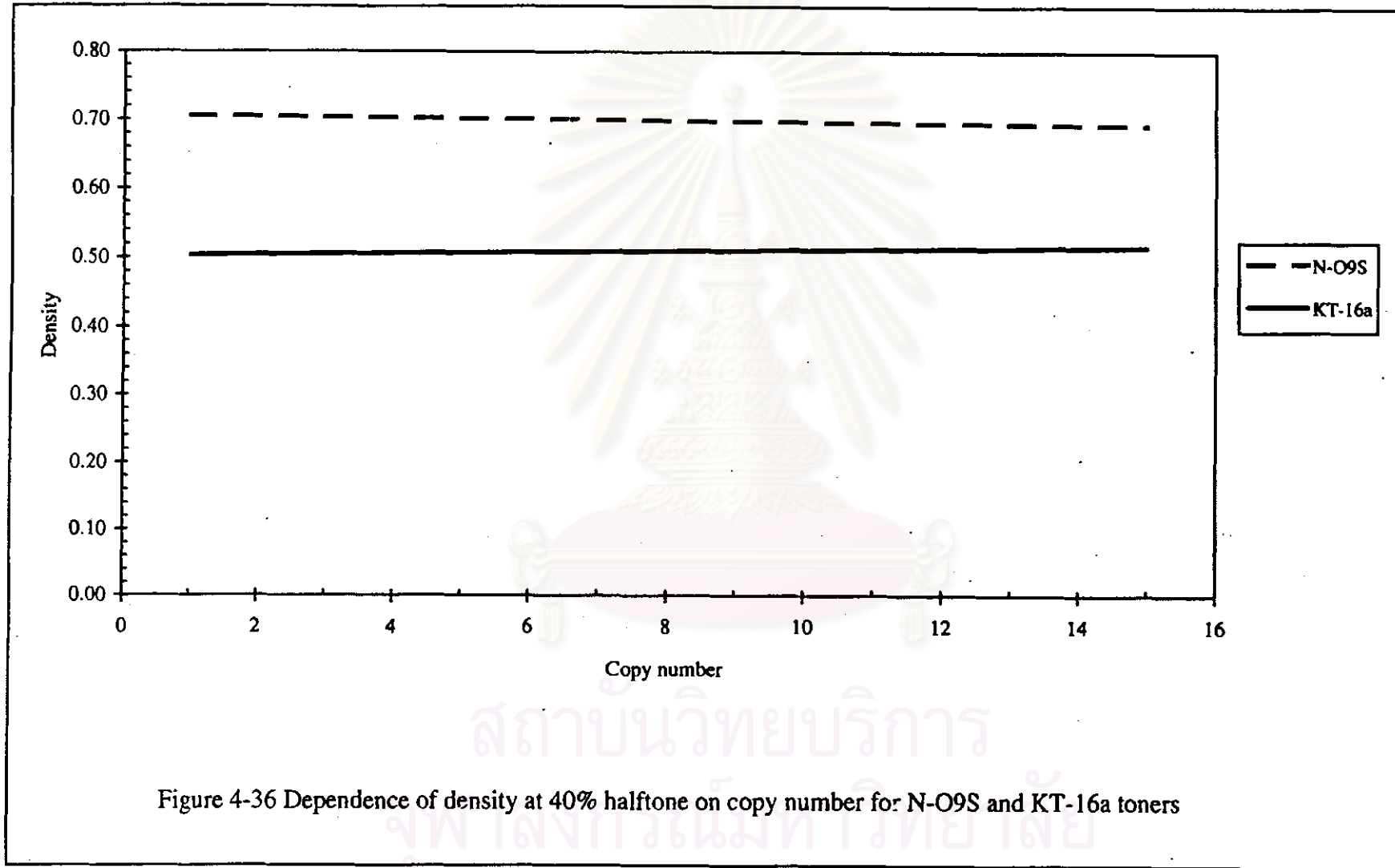


Figure 4-36 Dependence of density at 40% halftone on copy number for N-O9S and KT-16a toners

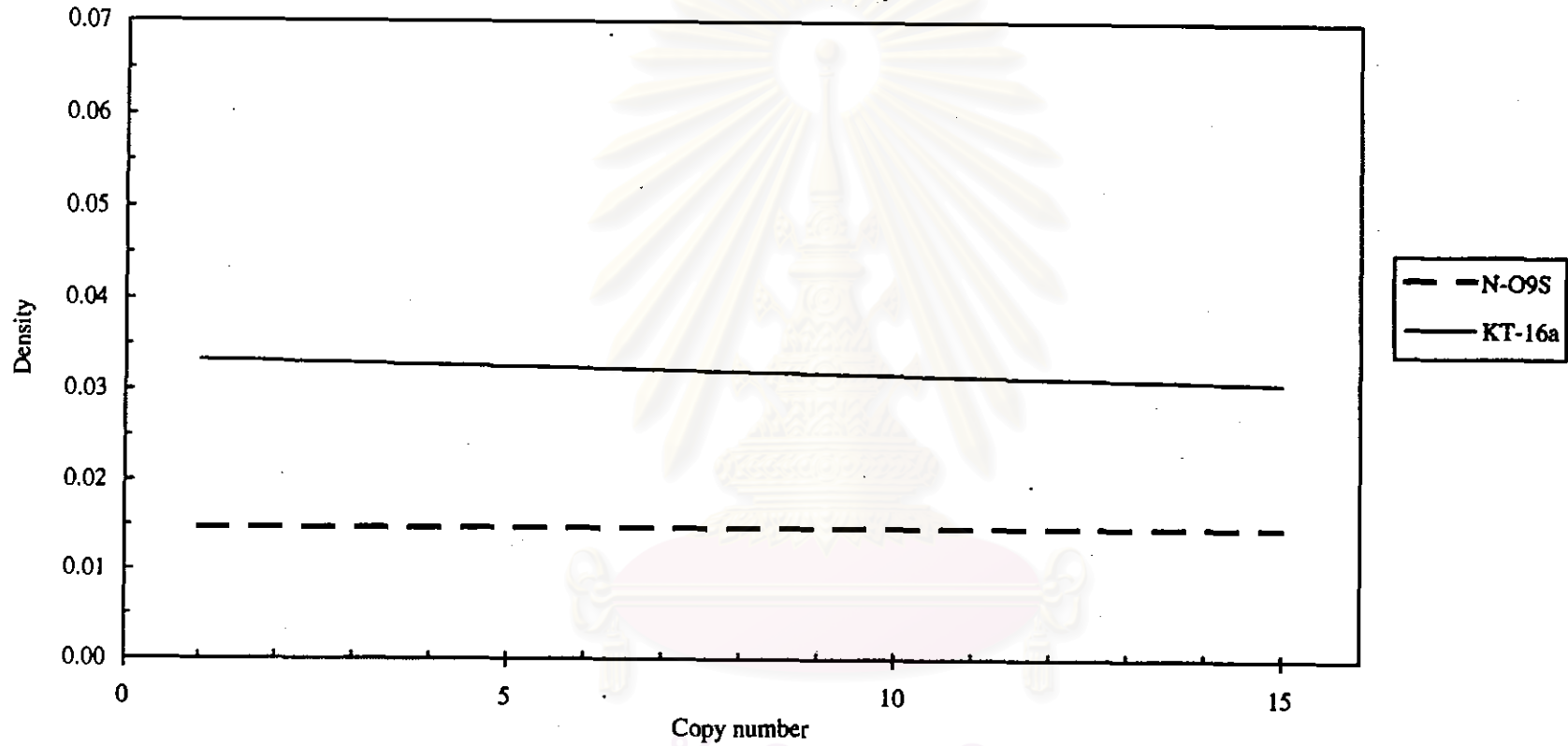


Figure 4-37 Dependence of background density on copy number for N-09S and KT-16a toners

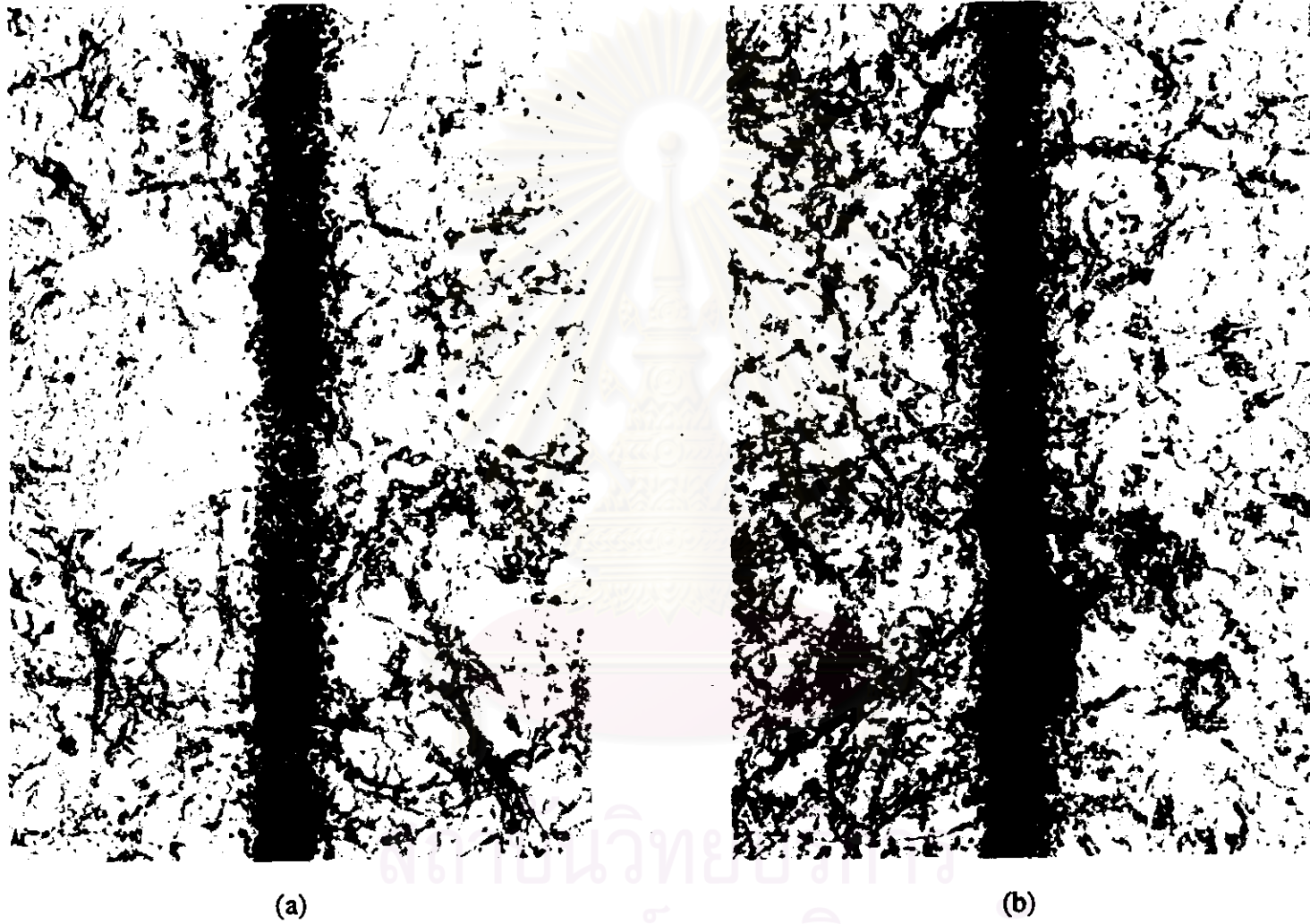


Figure 4-38 The photos of the lines (left side) by the image analyzer : (a) KT-16a toner and (b) N-O9S toner, (x400)

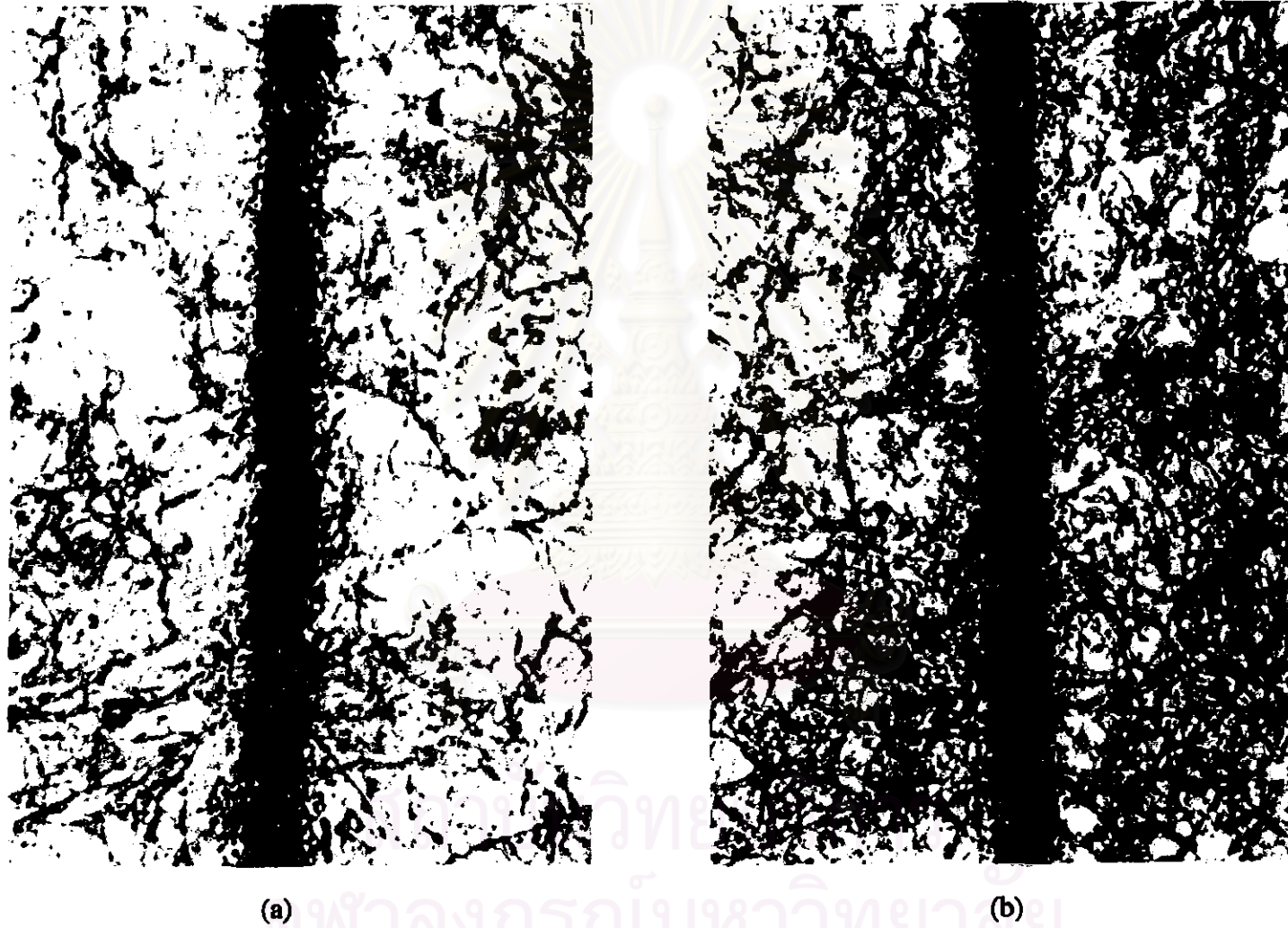


Figure 4-39 The photos of the lines (center) by the image analyzer : (a) KT-16a toner and (b) N-O9S toner, (x400)

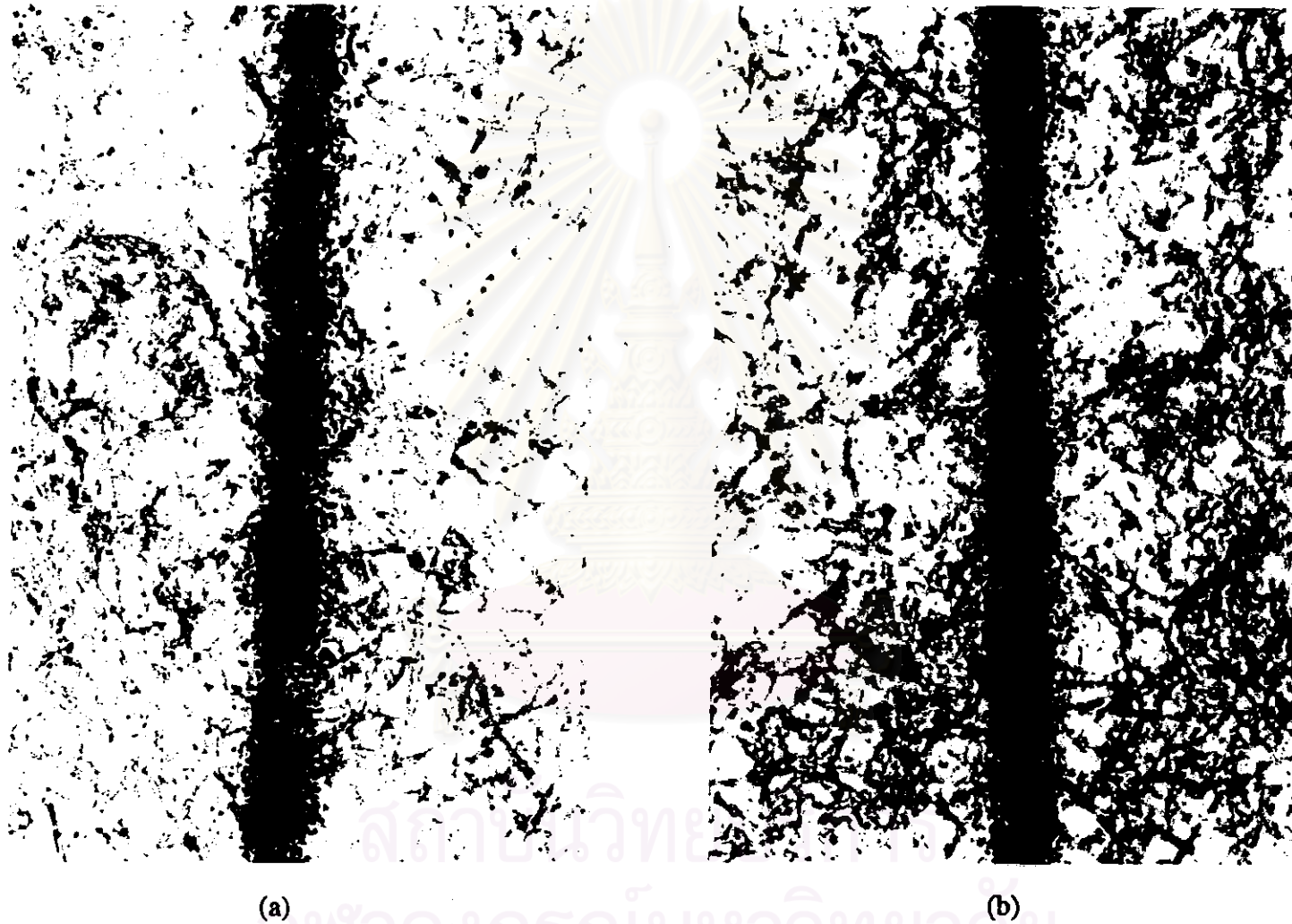


Figure 4-40 The photos of the lines (right side) by the image analyzer : (a) KT-16a toner and (b) N-O9S toner, (x400)



(a)

(b)

Figure 4-41 The photos of the "a" character by the image analyzer : (a) KT-16a toner and (b) N-O9S toner, (x20)

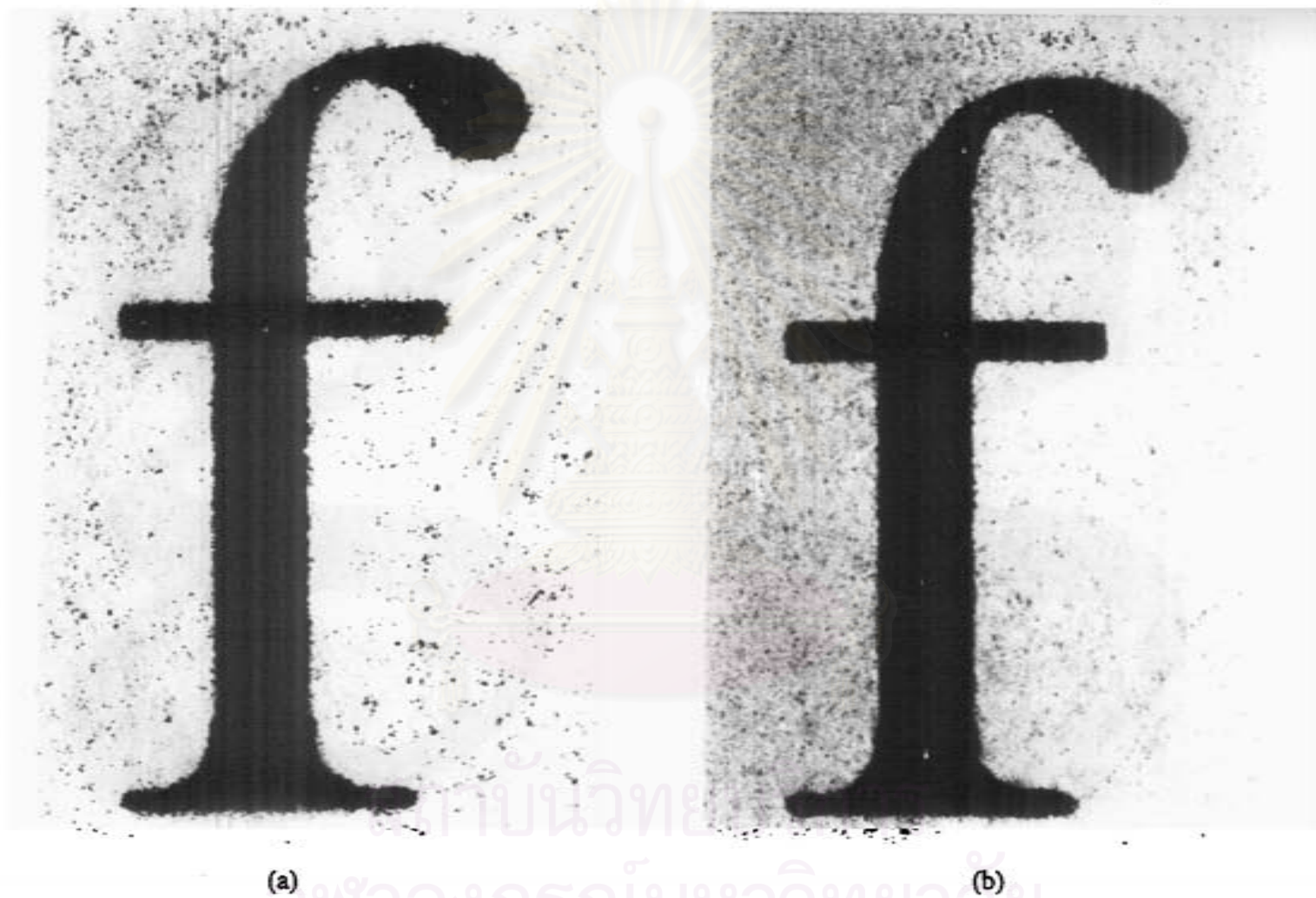
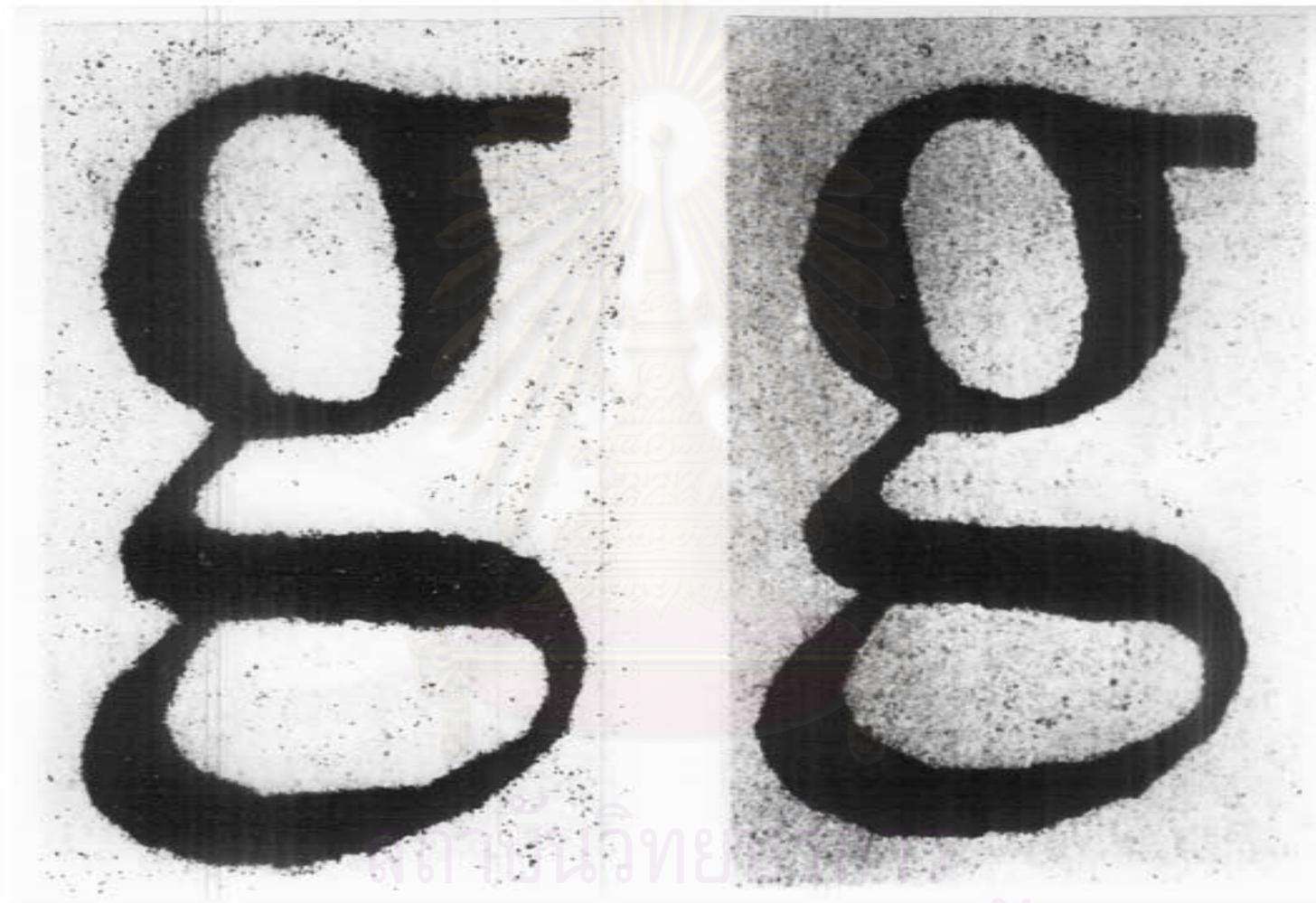


Figure 4-42 The photos of the "f" character by the image analyzer : (a) KT-16a toner and (b) N-09S toner, (x20)

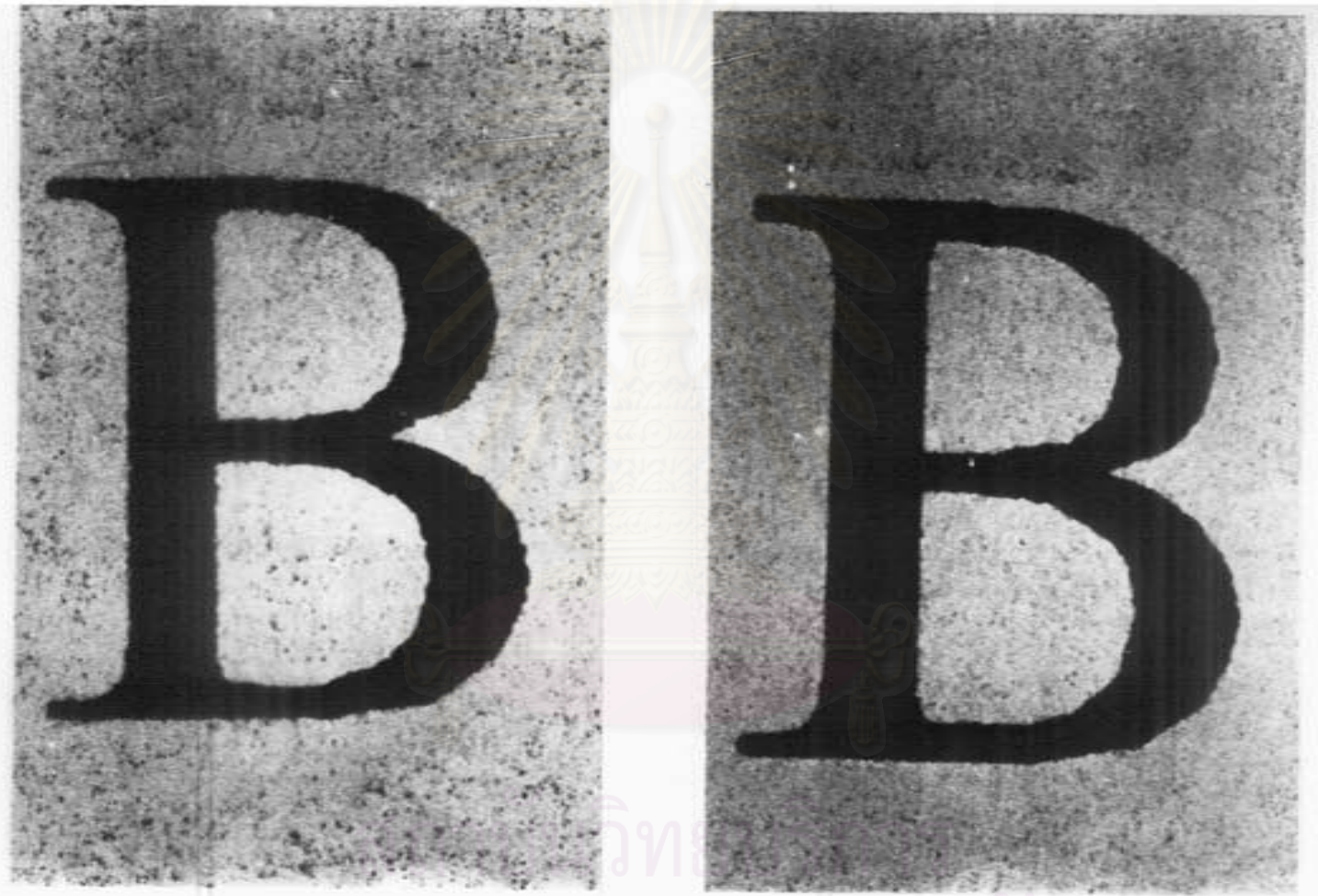


(a)

(b)

Figure 4-43 The photos of the "g" character by the image analyzer : (a) KT-16a toner and (b) N-09S toner, (x20)

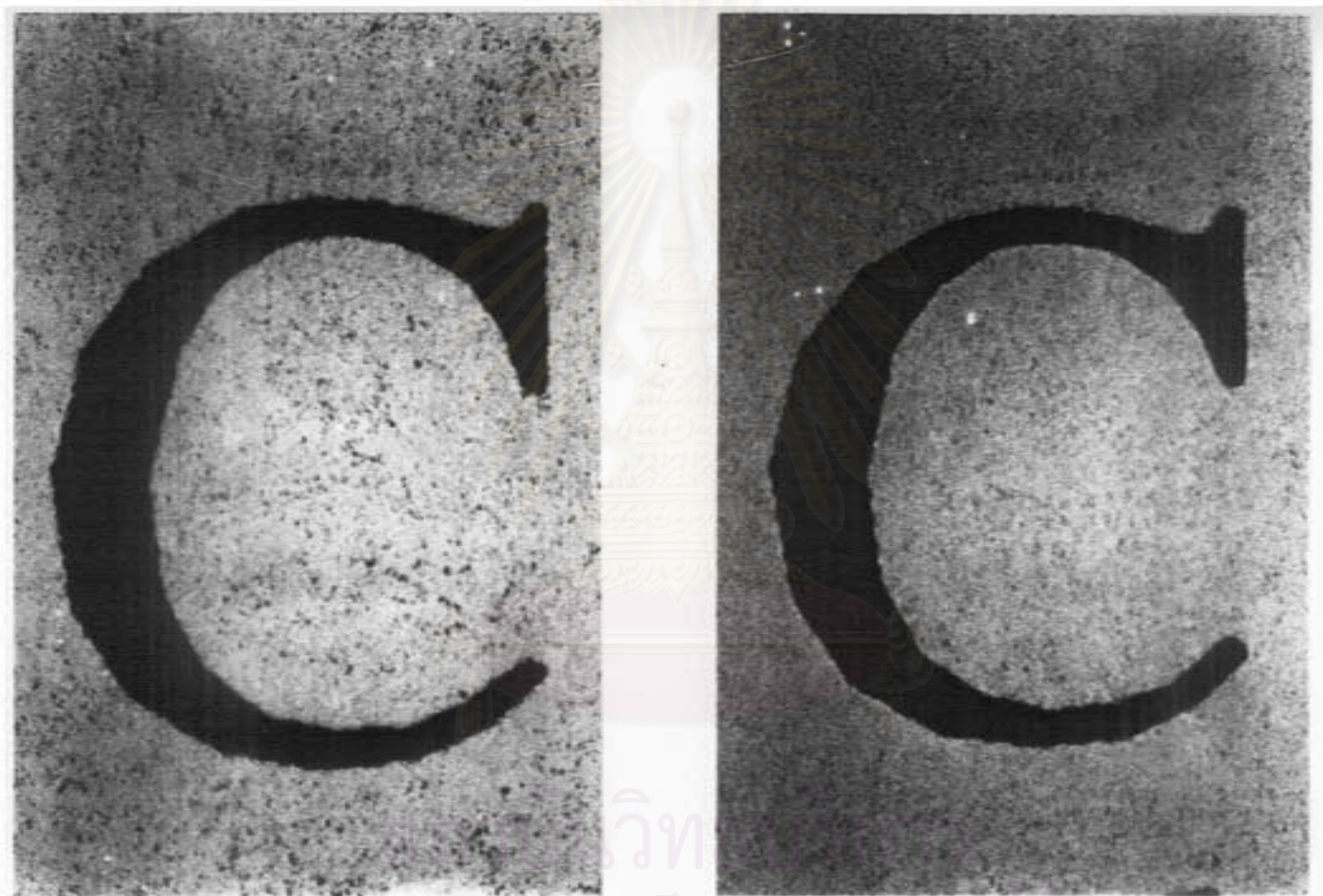




(a)

(b)

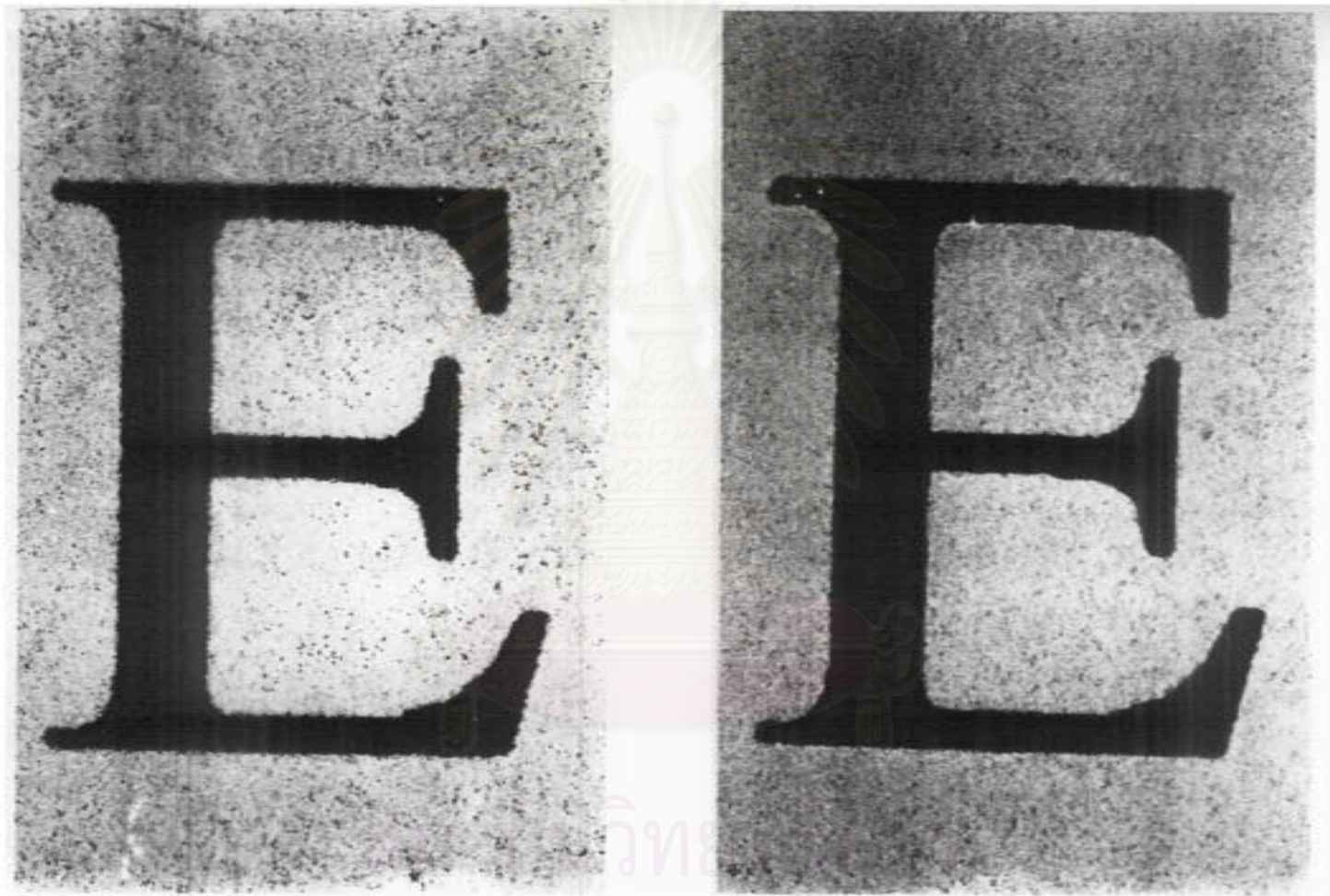
Figure 4-44 The photos of the "B" character by the image analyzer : (a) KT-16a toner and (b) N-O9S toner, (x15)



(a)

(b)

Figure 4-45 The photos of the "C" character by the image analyzer : (a) KT-16a toner and (b) N-O9S toner, (x15)



(a)

(b)

Figure 4-46 The photos of the "E" character by the image analyzer : (a) KT-16a toner and (b) N-09S toner, (x15)

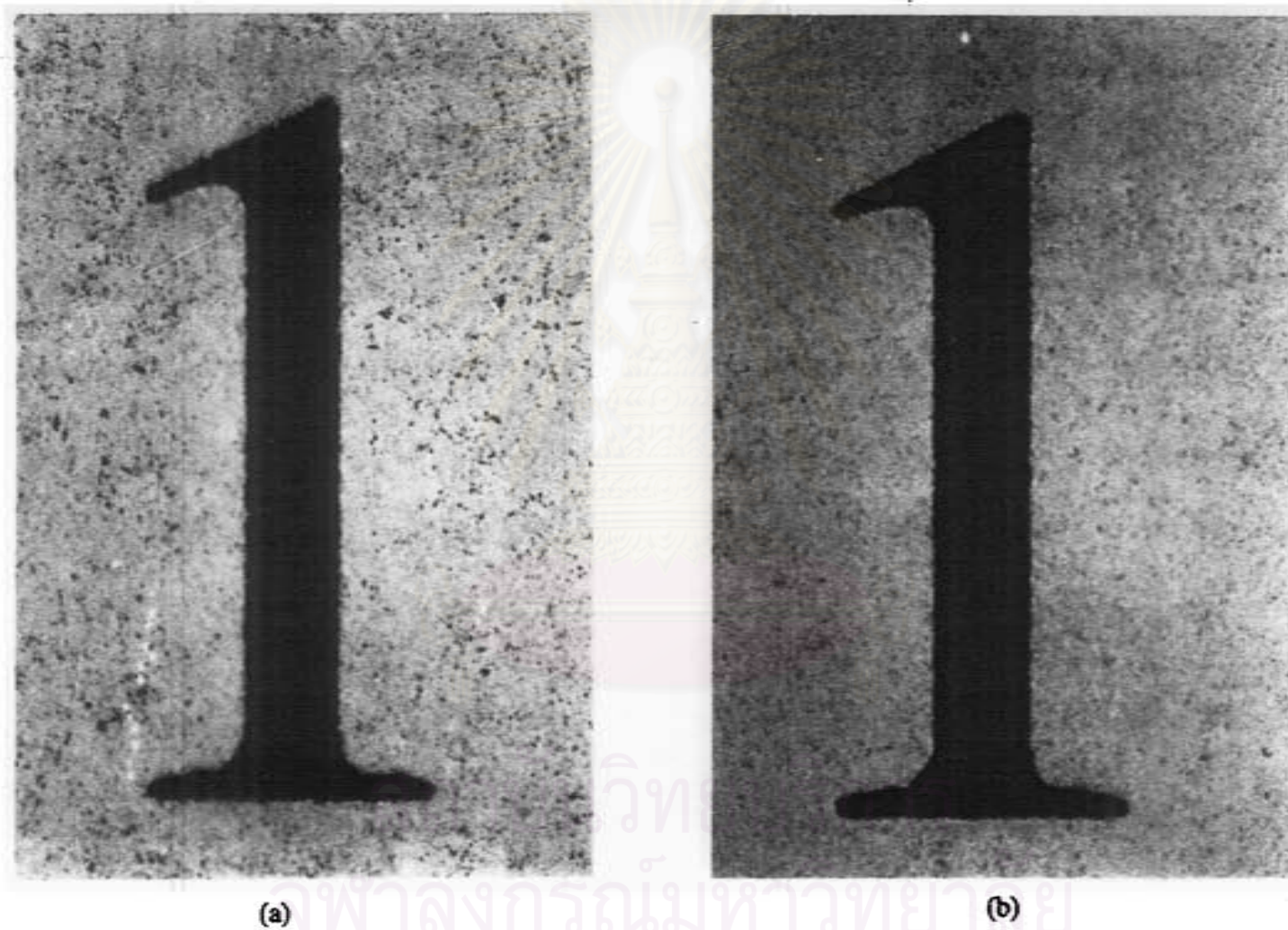
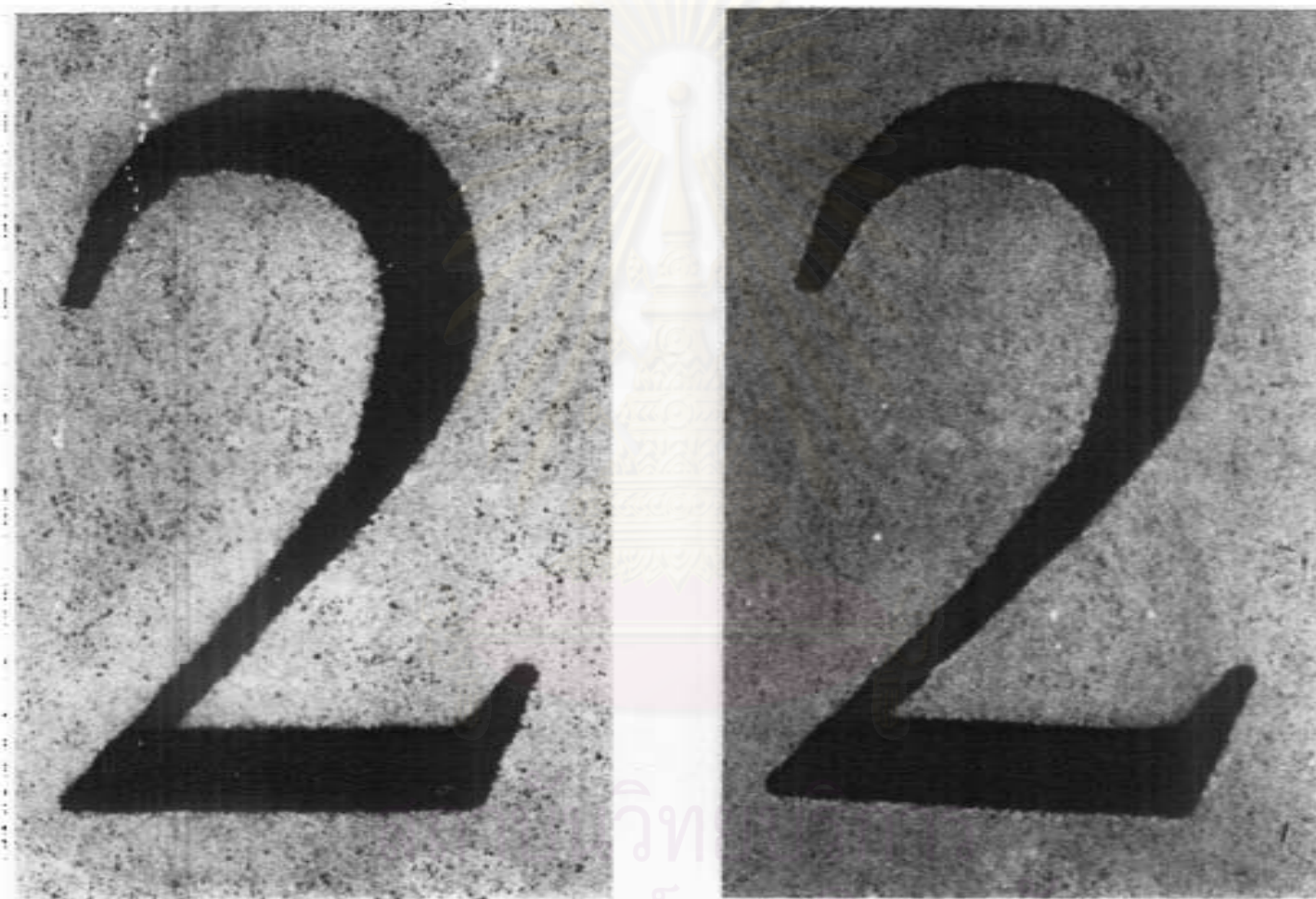


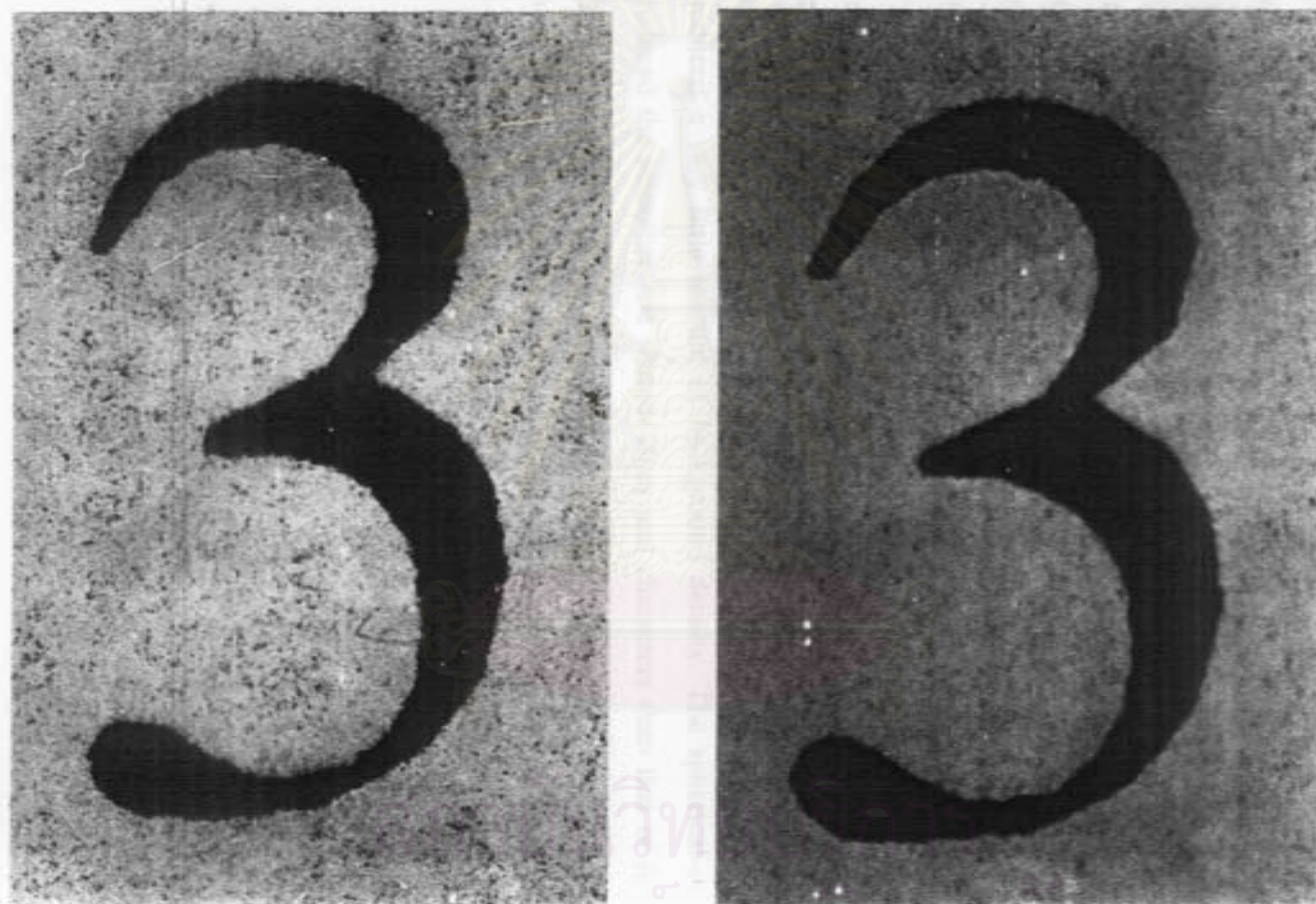
Figure 4-47 The photos of the "1" character by the image analyzer : (a) KT-16a toner and (b) N-O9S toner, (x20)



(a)

(b)

Figure 4-48 The photos of the "2" character by the image analyzer : (a) KT-16a toner and (b) N-09S toner, (x20)



(a)

(b)

Figure 4-49 The photos of the "3" character by the image analyzer : (a) KT-16a toner and (b) N-O9S toner, (x20)

Figures 4-38 to 4-49 show the lines (0.5 point) and the “a, f, g, B, C, E, 1, 2, and 3” characters of the N-O9S toner and KT-16a toner, respectively. For the KT-16a toner, the lines and the characters show background fog and raggedness. The N-O9S toner shows virtually no distortion of the character. The lines and the characters printed with spherical-shaped toner, N-O9S, were sharper and smoother than that of the irregularly-shaped toner, KT-16a. These results could be explained that the irregular-shaped toner contained the low charge toner. This low charge toner is picked up by the photoconductor drum, but is not transferred to the paper by electric field. On the other hand, the spherical-shaped toner is more efficiently and uniformly triboelectrically charged than the irregular-shaped toner. So, the spherical-shaped toner contained the high charge toner and could be transferred to the paper more than the other.<sup>26, 27</sup>

In conclusion, two types of toners, the KT-16a toner and the N-O9S toner, produced the high print density at the solid density. For 40 and 60% halftones, the different density values were produced in that the density values of the copy printed with the N-O9S toner were higher than that of the KT-16a toner. Both toners produced a very little amount of background density. The spherical-shaped toner produced the smoother and sharper lines and characters than that of the irregular-shaped toner. The irregular-shaped toner had the background fog and edge raggedness than the other.

สถาบันวิทยบริการ  
จุฬาลงกรณ์มหาวิทยาลัย